AD NUMBER
AD005010
CLASSIFICATION CHANGES
TO: unclassified
FROM: confidential
LIMITATION CHANGES
TO: Approved for public release, distribution unlimited
FROM: Distribution authorized to U.S. Gov't. agencies and their contractors; Administrative/Operational Use; Oct 1952. Other requests shall be referred to Wright Air Development Center, Wright-Patterson AFB, OH 45433.
AUTHORITY
31 Oct 1964, DoDD 5200.10; AFAL ltr, 17 Aug 1979

[redacted]

WADC TECHNICAL REPORT 52-278

SECURITY INFORMATION

INVESTIGATION OF THE ACCELERATION AND JOLT HISTORIES DURING ESCAPE FROM HIGH SPEED AIRCRAFT

MAX G. SCHERBERG
HARRY FERGUSON

FLIGHT RESEARCH LABORATORY

OCTOBER 1952

Statement A
Approved for Public Release

WRIGHT AIR DEVELOPMENT CENTER

AF-WP-(B)-O-7 APR 53 100

[redacted]

NOTICES

When Government drawings, specifications, or other data are used for any purpose other than in connection with a definitely related Government procurement operation, the United States Government thereby incurs no responsibility nor any obligation whatsoever; and the fact that the Government may have formulated, furnished, or in any way supplied the said drawings, specifications, or other data, is not to be regarded by implication or otherwise as in any manner licensing the holder or any other person or corporation, or conveying any rights or permission to manufacture, use, or sell any patented invention that may in any way be related thereto.

The information furnished herewith is made available for study upon the understanding that the Government's proprietary interests in and relating thereto shall not be impaired. It is desired that the Judge Advocate (WCJ), Wright Air Development Center, Wright-Patterson Air Force Base, Ohio, be promptly notified of any apparent conflict between the Government's proprietary interests and those of others.

[redacted]

INVESTIGATION OF THE ACCELERATION AND JOLT HISTORIES DURING ESCAPE FROM HIGH SPEED AIRCRAFT

Max G. Scherberg
Harry Ferguson

Flight Research Laboratory

October 1952

RDO No. 460-50-25

Wright Air Development Center
Air Research and Development Command
United States Air Force
Wright-Patterson Air Force Base, Ohio

[redacted]

[redacted]

FOREWORD

This report was prepared in the Mathematics Research Branch, Flight Research Laboratory, Wright Air Development Center, Air Research and Development Command under RDO No. 460-50-25, "Mathematical Investigation of Pilot Escape from High Speed Aircraft." Harry Ferguson acted as project engineer.

[redacted]

[redacted]

ABSTRACT

It is shown that the maximum acceleration that a person may encounter at a given time after separation of his escape unit from a damaged, unrecoverable aircraft is dependent only on the velocity of the aircraft. Acceleration histories determined from flight tests indicate that these theoretical maximums are reasonable and practical at least in the subsonic case.

Lt. Colonel J. P. Stapp of the Aero Medical Laboratory has reported (see paragraph 3) that high rate of acceleration onset during a fixed time produces injuries not found at lower onset rates. On the hypothesis that decay rates may be of comparable interest it is shown in this report that decay acceleration rates are functions of the initial acceleration and speed of the escape unit.

The accelerations parallel to and normal to the spine of a person in a tumbling escape unit are calculated for an assumed hypothetical case. The effects of these alternately increasing and decreasing accelerations on the person may be described as a shaking phenomena which may be beneficial to the escaping person.

The security classification of the title of this report is UNCLASSIFIED.

PUBLICATION REVIEW

This report has been reviewed and is approved.

FOR THE COMMANDING GENERAL:

Leslie B. Williams

LESLIE B. WILLIAMS
Colonel, USAF
Chief, Flight Research Laboratory
Directorate of Research

[redacted]

[redacted]

TABLE OF CONTENTS

[redacted]

LIST OF SYMBOLS

t = time (seconds) measured from the instant of separation of escape unit

x = distance (feet) travel of the escape unit

$\dot{x}$, $\ddot{x}$ = speed and acceleration, respectively after t seconds

$\dot{x}_o$, $\ddot{x}_o$ = speed and acceleration respectively at separation time t = o

S = effective drag area of the escape unit

C_D = drag coefficient of escape unit (considered constant in this study)

W = weight (pounds) of escape unit

h = altitude (feet) above sea level

ρ = density (slugs/ft^3) of atmosphere

$\left|\dddot{x}\right| = \left|\frac{d\ddot{x}}{dt}\right|$ = jolt measure

[redacted]

INTRODUCTION

The nature of the accelerations and jolts that a pilot may expect to encounter during escape from a damaged, unrecoverable, high speed aircraft would appear to depend on many conditions such as vehicle of escape, speed of the aircraft, altitude of the aircraft, motion during escape, mass of escape unit, and the method of holding the pilot in the escape unit. These conditions and the physical and psychological tolerances of humans to accelerations determine design criteria for escape mechanisms and associated aircraft.

Although all the factors mentioned above are not treated in this report, the major part of them are considered and the relative importance of these several parameter conditions is indicated. This study does not consider the process or the effect of the build up to the peak acceleration.

[redacted]

1. Calculation of speed and acceleration histories during escape.

Since the accelerations of primary interest will be of short duration (less than five seconds) and of orders of magnitude above 2g, the gravitational force component which in general will be essentially normal to the path has been ignored in this study. Also no attempt is made to take into account the effect of pitching, pitch attitude and acceleration on the drag coefficient. It has been anticipated that compressibility will not cause abrupt changes in drag at initiating speeds below the transonic and during the escape period of interest. For initiating speeds at or above transonic speed a discontinuous or abrupt change in drag may be expected and therefore the results are subject to correction for this effect. A subsequent study will treat this matter. Under the conditions specified the equation of motion becomes.

$$(1)\quad \ddot{x} = -K\,\dot{x}^2$$

in which K is a positive constant. This equation has solutions defining the time histories of speed and acceleration of the escape unit. These are

$$(2)\quad \frac{\dot{x}}{\dot{x}_o} = \frac{1}{1 - \frac{\ddot{x}_o}{\dot{x}_o}\,t} \qquad (\ddot{x}_o \text{ is negative})$$

and

$$(3)\quad \frac{\ddot{x}}{\ddot{x}_o} = \frac{1}{\left(1 - \frac{\ddot{x}_o}{\dot{x}_o}\,t\right)^2}$$

It is of interest to note how these histories depend on the initial speeds and accelerations. The decay rates of the speed and acceleration depend only on the ratio $\frac{\ddot{x}_o}{\dot{x}_o}$ and the latter is more rapid than the former.

2. Estimated Upper Bounds.

As has been indicated in the introductory remarks a multiplicity of escape conditions may generally be anticipated and it is desirable to develop overall information which depends on as few as possible of these parameters. This has been accomplished in this instance by calculating the maximum acceleration that may be expected at some given time t after initiation of escape.

For a given t and escape speed $\dot{x}_o$ the maximum acceleration that may be expected is found by setting the derivative of $\ddot{x}$ with respect to $\ddot{x}_o$ equal to

zero and solving for $\ddot{x}_o$ in terms of t and $\dot{x}_o$.

We have

$$(4) \qquad \frac{d\ddot{x}}{d\ddot{x}_o} = \frac{\dot{x}_o^2}{(\dot{x}_o - \ddot{x}_o t)^2} + \frac{2t\ddot{x}_o\dot{x}_o^2}{(\dot{x}_o - \ddot{x}_o t)^3}$$

$$= \frac{\dot{x}_o^2(\dot{x}_o + \ddot{x}_o t)}{(\dot{x}_o - \ddot{x}_o t)^3}$$

and thus the $\ddot{x}_o$ which provides this is evidently

$$(5) \qquad \ddot{x}_o = -\frac{\dot{x}_o}{t}$$

and from (3) the maximum acceleration takes the form

$$(6) \qquad \max|\ddot{x}| = \frac{\dot{x}_o}{4t}$$

Clearly this result is independent of weight of escape unit, drag coefficient, effective drag area, and altitude of escape. From (5) it is also clear that the $\max|\ddot{x}|$ is always attained at some time during escape for each initial escape speed.

Equation (6) thus provides upper bounds for acceleration histories during escape which depend only on the initial velocity of escape. Of course these upper bounds are not practical for values of t close to zero and an alternate method is used for these small time values. Figures 1, 2, and 3 show graphs of (6) for the time interval 0.5 to 4.0 seconds and for initial speeds at 200 MPH intervals, from 400 MPH to 1800 MPH.

Figure 1 shows a pair of acceleration histories determined from flight tests. These curves when compared with the theoretical curves indicate that the latter are reasonable and practical upper bounds in the subsonic case of acceleration histories over a wide range of escape conditions (for more detail see paragraph 4 below). It should be noted however that these curves include speeds which are subsonic, transonic, and supersonic and that the equation of motion (1) is not completely applicable for motions initiated at supersonic and transonic speeds. Attempts to obtain more quantitative information in these cases are in process.

The following method was used to establish upper acceleration bounds in the time interval 0.0 to 0.5. At t = o we have

$$(7)\quad \ddot{x}_o = -\frac{gSC_D P\dot{x}_o^2}{2W}$$

Examination of experimental results indicate that 1/30 may be used for an upper bound for $\frac{S\,C_D}{W}$ and hence

$$(8)\quad \ddot{x}_o \quad \frac{1}{60} \quad \dot{x}_o^{\,2} g$$

The upper bound at t=o is estimated by (8) for a specified altitude and was joined by a straight line segment to the upper bound at t=0.5 estimated by (6). This line segment determines conservatively the upper bound for the time interval $0.0 \leq t \leq 0.5$ and for the specified altitude as a minimum altitude. Since this result depends on the density altitude the results as presented in figures 1, 2, and 3 correspond in this time interval 0.0 to 0.5 seconds to the minimum altitudes there indicated.

When using the graphs in figures 1-3 it is important to bear in mind that the acceleration man can tolerate is dependent on the time interval and the specific attitude of the man during the acceleration. Man can tolerate higher acceleration for shorter time intervals, and can endure greater accelerations in directions normal to the spine than in directions parallel to the spine. In the direction parallel to the spine, man can stand greater acceleration in the direction toward the head (blood flows from the head causing black out) than he can stand in the direction away from the head (blood flows to the head and may cause red out).

3. The Jolt.

It has been shown that the rate of onset of acceleration can produce serious injury to the submitting subject as reported in AF Technical Report No. 5915, "Human Exposures to Linear Deceleration, Part 2: The Forward-Facing Position and the Development of a Crash Harness" by Major John Paul Stapp. This effect is defined as a jolt and the third derivative $\dddot{x}$ has been adopted as its measure. Using the same measure for deceleration decay effect and again assuming that equation (1) is applicable, that is, that the drag force is proportional to the square of the speed, one finds readily that

$$(9)\quad \dddot{x} = \frac{2\ddot{x}_o^{\,2}\dot{x}_o^{\,2}}{(\dot{x}_o - \ddot{x}_o t)^3}$$

Since $\ddot{x}_o$ is negative it is obvious that $\dddot{x}$ is a maximum when t=o and hence

$$(10)\quad \dddot{x}_{max} = \frac{2\ddot{x}_o^{\,2}}{\dot{x}_o}$$

Figure (4) shows graphs of (10). The graphs show the jolt as a function of the initial acceleration, for initial speeds at 200 MPH intervals for a range from

400 MPH to 1800 MPH. The graphs for initial velocities of 400, 600 and 800 MPH were cut off at values of $\ddot{x}_o$ which correspond to the upper bounds of $\dddot{x}$ estimated at t=0. The other curves would have correspondingly been cut off if the $\ddot{x}_o$ scale had extended sufficiently far beyond 76g.

It should be noted that, contrary to the upper bound results, jolt results are probably valid at both the transonic and supersonic speeds. On the other hand they measure only the jolt due to acceleration decay and give no information about onset effects.

It is interesting to note that for a given initial acceleration $\ddot{x}_o$ condition the jolt decreases with increase in initial speed and that for a given initial speed the jolt increases with increase in initial acceleration. Thus an aerodynamic clean up of the escape unit will reduce jolt while a reduction in weight will increase jolt.

4. Experimental Data Shows Maximum Decelerations and Jolts are Nearly Attained.

An investigation was made to determine the accelerations encountered in tests of seat ejections carried on at Muroc and Hamilton Air Force Bases. These tests are reported in Memorandum Report, MR#MCREXA7-45341-4-1, Pilot Ejection Flight Tests Conducted with a TF-80C Airplane at Muroc and Hamilton Air Force Bases. Graphs of the paths of the ejections are given in the report. Using the graphs of Test No. 22, Page 27, live test (Captain V. Mazza), and Test No. 36, Page 41, dummy test, horizontal and vertical accelerations were determined mathematically. The graphs of these are plotted on figure 1, and the maximum jolts encountered are marked on figure 4. It is observed that the experimental values of acceleration and jolt attain values very near the theoretical maximums.

5. Explanation of the Graphs of $\ddot{x}$ as a Function of $\dddot{x}_o$.

Graphs (figures 5-7) have been drawn using $\ddot{x} = \frac{\ddot{x}_o \dot{x}_o^2}{(\dot{x}_o - \ddot{x}_o t)^2}$ for t = $\frac{1}{2}$, 1, 2, 3, and $\dot{x}_o$ = 400, 800 and 1200 MPH and letting $\ddot{x}_o$ vary. It is of interest to note that for a given time t, a given velocity of the aircraft, and for a given acceleration of the man there are two initial accelerations. For example, figure 6, if $\dot{x}_o$ = 800 MPH there are two initial accelerations -8g and -38g which give an acceleration of -4g when t = 2. The relationship between values of time, velocity of the aircraft, and the two initial accelerations $\ddot{x}_o$ and $\ddot{x}_{oo}$ is obtained by solving

$$\frac{\ddot{x}_o \dot{x}_o^2}{(\dot{x}_o - \ddot{x}_o t)^2} = \frac{\ddot{x}_{oo} \dot{x}_o^2}{(\dot{x}_o - \ddot{x}_{oo} t)^2}$$

400 MPH to 1800 MPH. The graphs for initial velocities of 400, 600 and 800 MPH were cut off at values of $\ddot{x}_o$ which correspond to the upper bounds of $\ddot{x}$ estimated at t=0. The other curves would have correspondingly been cut off if the $\ddot{x}_o$ scale had extended sufficiently far beyond 76g.

It should be noted that, contrary to the upper bound results, jolt results are probably valid at both the transonic and supersonic speeds. On the other hand they measure only the jolt due to acceleration decay and give no information about onset effects.

It is interesting to note that for a given initial acceleration $\ddot{x}_o$ condition the jolt decreases with increase in initial speed and that for a given initial speed the jolt increases with increase in initial acceleration. Thus an aerodynamic clean up of the escape unit will reduce jolt while a reduction in weight will increase jolt.

4. Experimental Data Shows Maximum Decelerations and Jolts are Nearly Attained.

An investigation was made to determine the accelerations encountered in tests of seat ejections carried on at Muroc and Hamilton Air Force Bases. These tests are reported in Memorandum Report, MR#MCREXA7-45341-4-1, Pilot Ejection Flight Tests Conducted with a TF-80C Airplane at Muroc and Hamilton Air Force Bases. Graphs of the paths of the ejections are given in the report. Using the graphs of Test No. 22, Page 27, live test (Captain V. Mazza), and Test No. 36, Page 41, dummy test, horizontal and vertical accelerations were determined mathematically. The graphs of these are plotted on figure 1, and the maximum jolts encountered are marked on figure 4. It is observed that the experimental values of acceleration and jolt attain values very near the theoretical maximums.

5. Explanation of the Graphs of $\ddot{x}$ as a Function of $\dddot{x}_o$.

Graphs (figures 5-7) have been drawn using $\ddot{x} = \frac{\ddot{x}_o \dot{x}_o^2}{(\dot{x}_o - \ddot{x}_o t)^2}$ for t = $\frac{1}{2}$, 1, 2, 3, and $\dot{x}_o$ = 400, 800 and 1200 MPH and letting $\ddot{x}_o$ vary. It is of interest to note that for a given time t, a given velocity of the aircraft, and for a given acceleration of the man there are two initial accelerations. For example, figure 6, if $\dot{x}_o$ = 800 MPH there are two initial accelerations -8g and -38g which give an acceleration of -4g when t = 2. The relationship between values of time, velocity of the aircraft, and the two initial accelerations $\ddot{x}_o$ and $\ddot{x}_{oo}$ is obtained by solving

$$\frac{\ddot{x}_o \dot{x}_o^2}{(\dot{x}_o - \ddot{x}_o t)^2} = \frac{\ddot{x}_{oo} \dot{x}_o^2}{(\dot{x}_o - \ddot{x}_{oo} t)^2}$$

for $\bar{t}$. One obtains $\bar{t} = \frac{\dot{x}_o}{\sqrt{\ddot{x}_o \ddot{x}_{oo}}}$ where $\bar{t}$ is the time when both accelerations are equal:

From the above information and graphs one concludes that for two ejections A and B at same initial velocity and initial accelerations $\ddot{x}_o$, $\ddot{x}_{oo}$ respectively, where $\ddot{x}_o$ is greater than $\ddot{x}_{oo}$, that at some instant $\bar{t}$ the accelerations are equal and prior to $\bar{t}$ the acceleration of A is greater than that of B and after $\bar{t}$ the acceleration of B is greater than that of A.

6. Acceleration Estimates for a Tumbling Escape Unit.

Some preliminary acceleration calculations on a tumbling escape unit have been made, based on simplifying assumptions concerning the nature of the tumbling and the drag coefficient during tumbling. Figure I below defines the basic geometry considered.

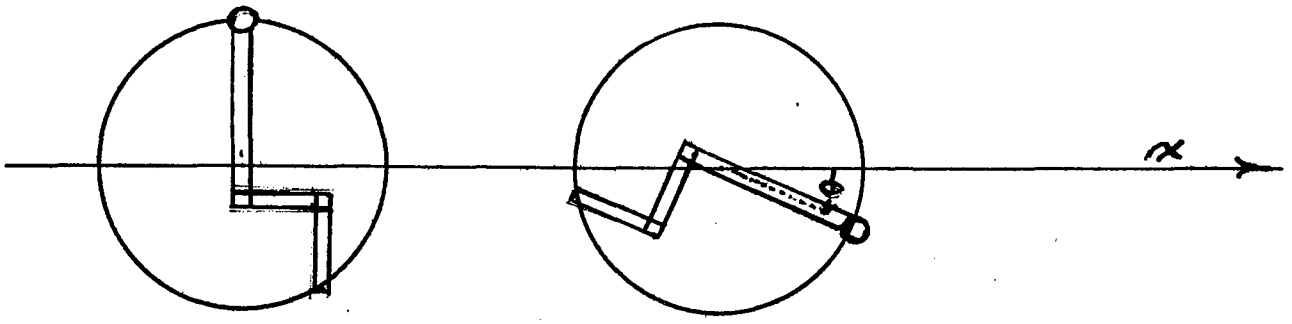

Fig. I

The vector labeled x defines the displacement of the c.g. of the escape unit in the direction of the airstream. The angle θ is the angle between the person's spine line and the direction of motion, and $w=\dot{\theta}$ is the angular velocity of the persons spine line. r is the distance from the persons c.g. to the body point at which accelerations are being considered. F_N and F_T are respectively the acceleration components normal and parallel to the persons spine line of the acceleration at some given point in the body.

The tumbling history of the escape unit was arbitrarily defined to be $w = w_o (1 - e^{-.6t})$ in which w_o is the terminal angular velocity. The graph of the function is below.

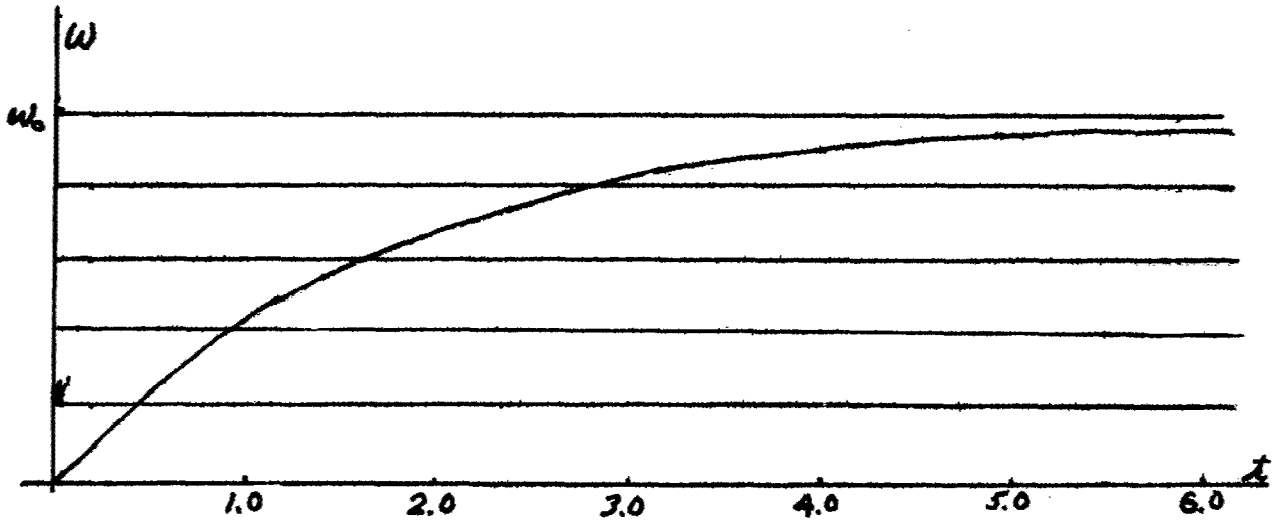

Accelerations F_N, F_T each consist of the sum of three accelerations due to linear accelerations of the person, rotation of the person, and the force of gravity on the person. The linear acceleration of the person is $\ddot{x} = \frac{\dot{x}_o \ddot{x}_o^2}{(\dot{x}_o - \ddot{x}_o t)^2}$ so its contribution to F_N is $\ddot{x}\cos\theta$ and to F_T is $-\ddot{x}\sin\theta$

It is assumed that accelerations in direction of stomach to head, and in direction of back to chest are positive. The rotational motion contributes to F_N an acceleration $-w^2\gamma = -w_o^2(1-e^{-.6t})^2\gamma$ and to F_T an acceleration of $\dot{w}\gamma = .6w_o\gamma e^{-.6t}$.

Force of gravity gives an acceleration of g sin θ to F_N and g cos θ to F_T. Therefore

$$F_N = \ddot{x}\cos\theta - w^2\gamma + g\sin\theta$$
$$F_T = -\ddot{x}\sin\theta + \dot{w}\gamma + g\cos\theta$$

Graphs have been drawn utilizing these formulas (figures 8-25). These graphs were drawn using the following values of the parameters:

$\dot{x}_o$ = 587(400 M.P.H.), $\ddot{x}_o$ = -440 , γ = 1, 2 and,

$w_o = \frac{10\pi}{3}$(100 r.p.m.), $\frac{5\pi}{3}$(50 r.pm.), $\frac{5\pi}{6}$ (25 r.p.m.)

Values of γ = 1, 2 are selected as representative of distance from center of rotation to the heart, and brain respectively of the person. Graphs are drawn of F_N(figures 8, 11, 14, 17, 20, 23) and F_T (figures 9, 12, 15, 18, 21, 24) as functions of t. To construct these graphs it is necessary to express θ as a function of t.

$$\frac{d\theta}{dt} = w$$
$$d\theta = w_o\,(1-e^{-.6t})\,dt$$

Integrate and use initial condition that $\theta = \theta_o$ when t=0 and obtain

$$\theta = \theta_o + w_o\left[t - \frac{5}{3}(1-e^{-.6t})\right]$$

Graphs shown in figures 10, 13, 16, 19, 22 and 25 show the actual vector acceleration that the tumbling escaping person would encounter. The effect might be described briefly as a shaking phenomenon. The damage that such a phenomenon might cause would be related to the natural frequencies of the body part concerned, the duration of the shake, and the frequency and amplitude of the shake.

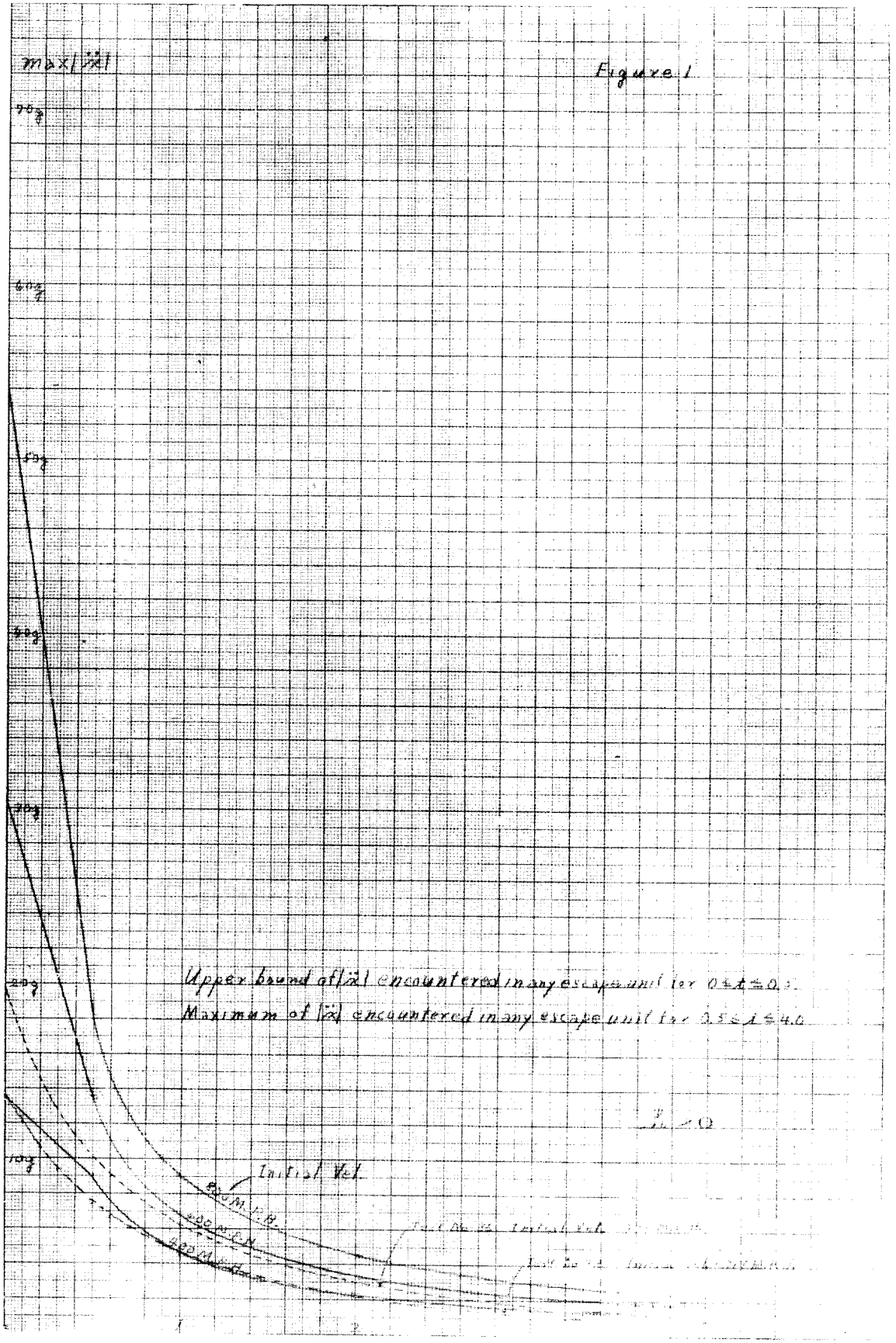
max|ẍ|
Figure 1
Upper bound of |ẍ| encountered in any escape unit for 0 ≤ t ≤ 0.5
Maximum of |ẍ| encountered in any escape unit for 0.5 ≤ t ≤ 4.0
Initial Vel.

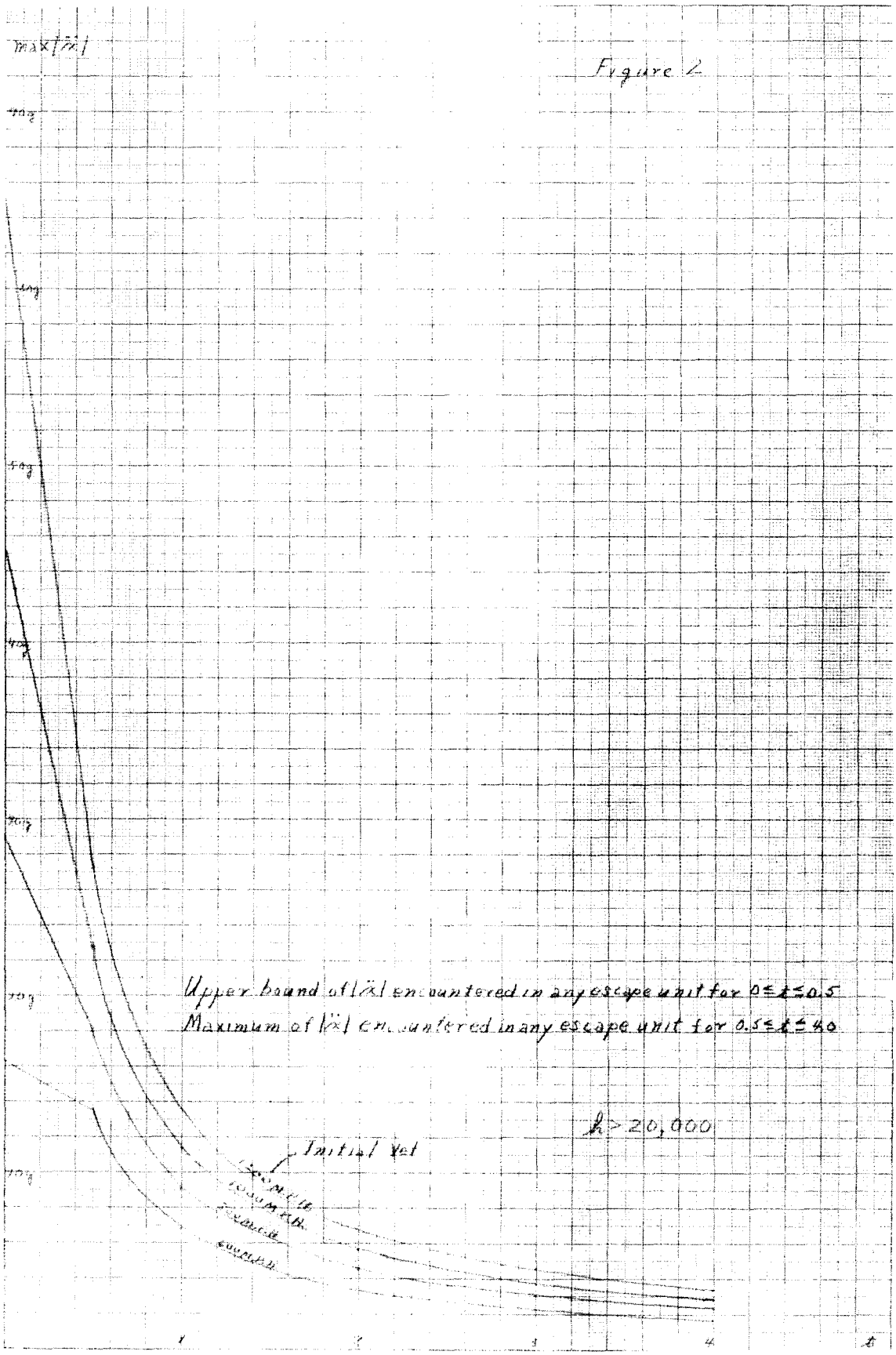
max[x̄i]
Figure 2
Upper bound of |x̄i| encountered in any escape unit for 0 ≤ t ≤ 0.5
Maximum of |x̄i| encountered in any escape unit for 0.5 ≤ t ≤ 40
h > 20,000
Initial val
1
2
3
4
t

Figure 3

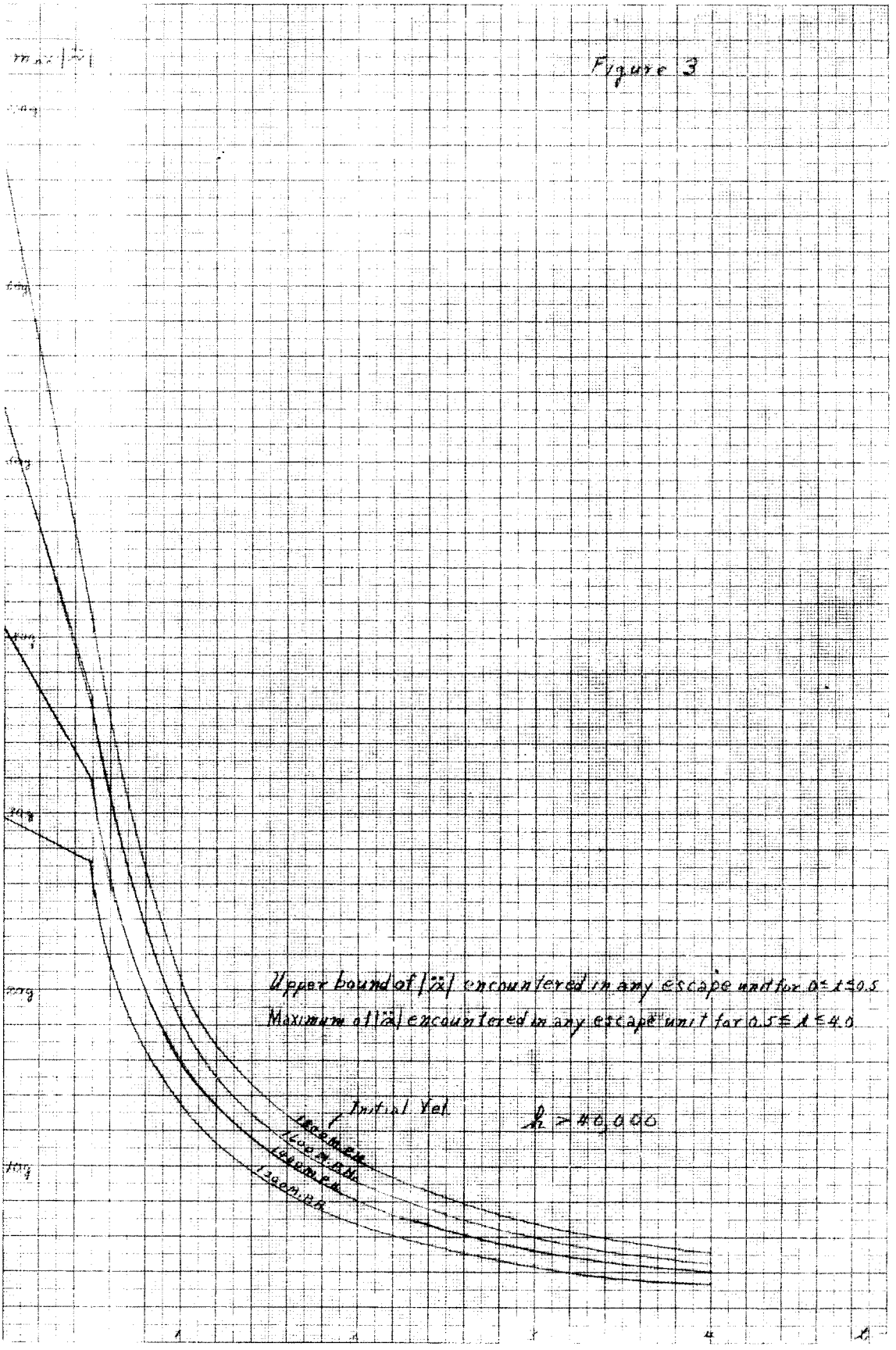
Upper bound of |ẍ| encountered in any escape unit for 0 ≤ t ≤ 0.5
Maximum of |ẍ| encountered in any escape unit for 0.5 ≤ t ≤ 4.0
Initial Vel
Increment
1 sec
2 sec
3 sec

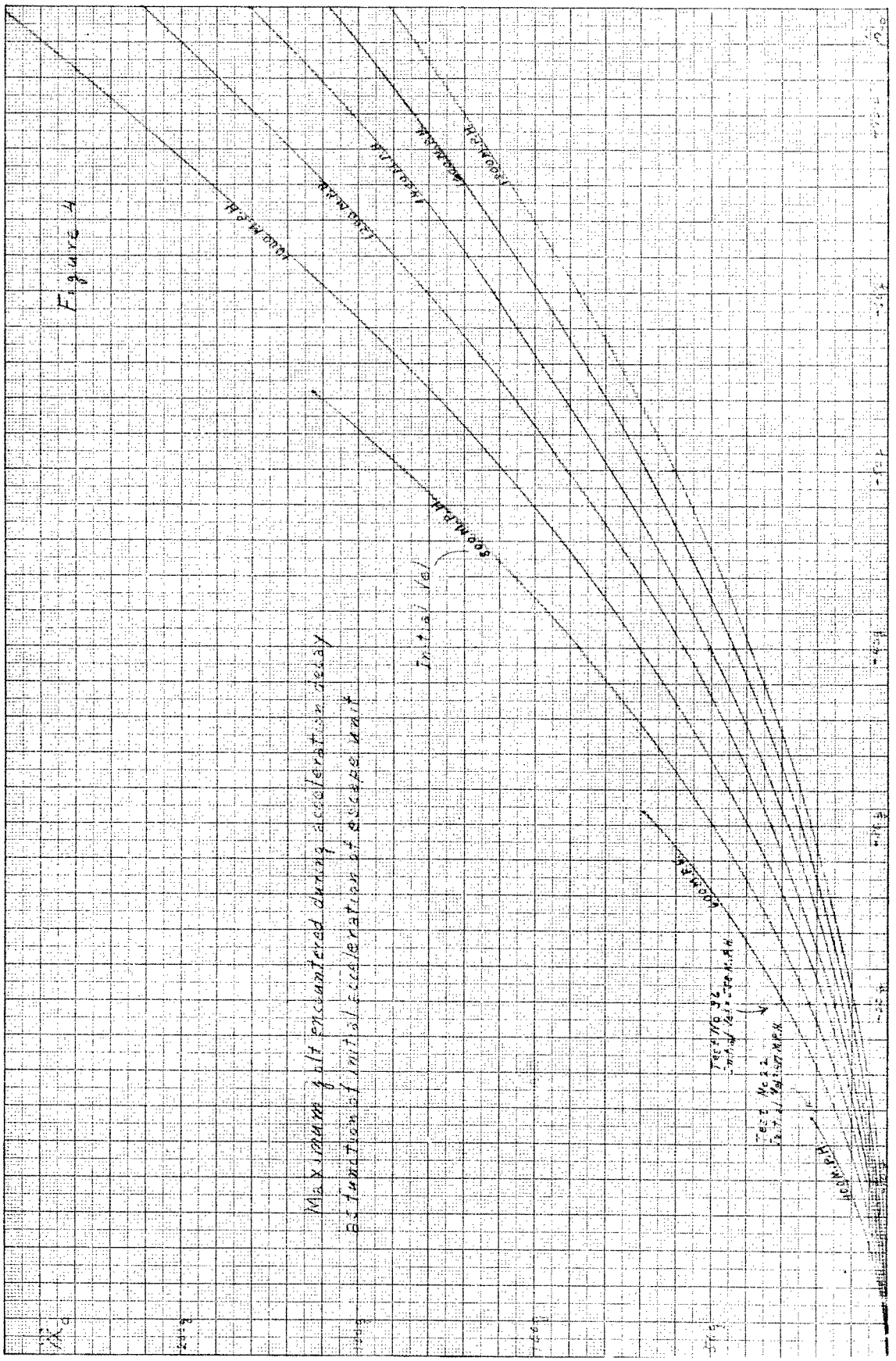
Figure 4
Maximum g-lift encountered during deceleration decay
as function of initial deceleration at release and
Initial (g)
8.0 g
7.0 g
6.0 g
5.0 g
4.0 g
3.0 g
Test No. 92
Test No. 93

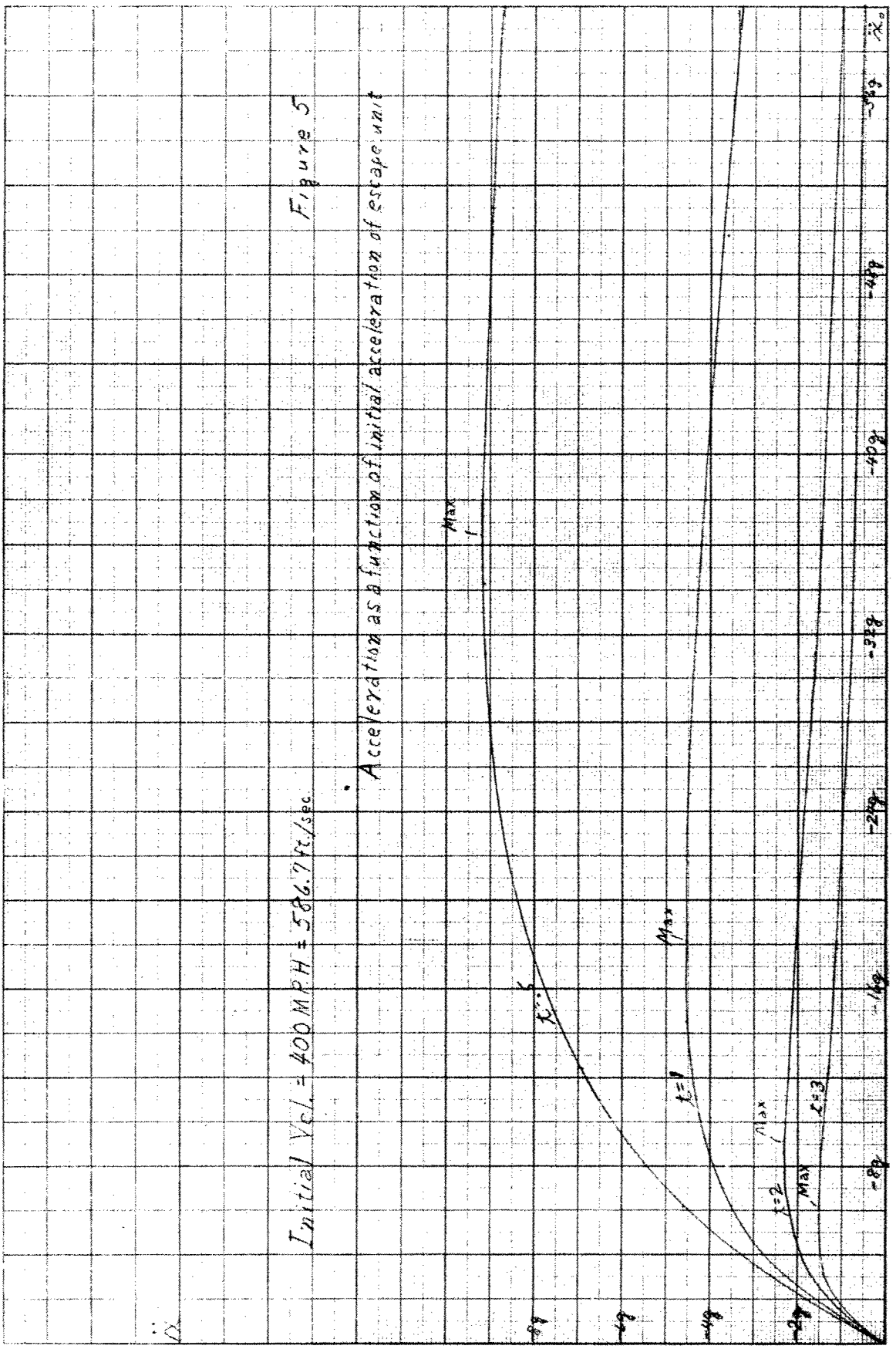
Figure 5
Acceleration as a function of initial acceleration of escape unit
Initial Vel = 400 MPH = 586.7 Ft./sec
Max
t=1
t=2
t=3
-8g
-4g
-2g
-1g

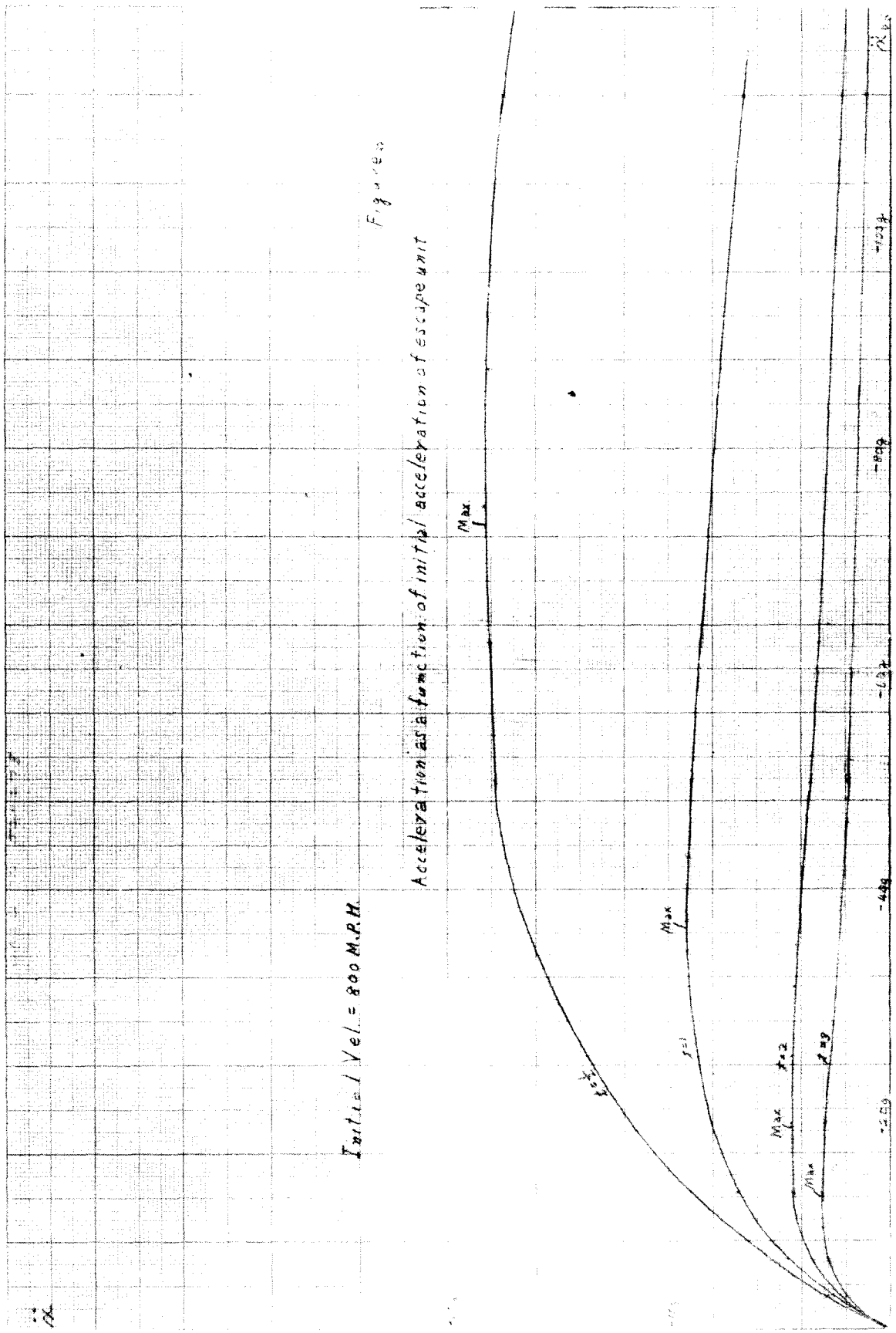
Figure
Acceleration as a function of initial acceleration of escape unit
Initial Vel = 800 M.P.H.
Max
Max
Max
Max
-400
-600
-800
-1000

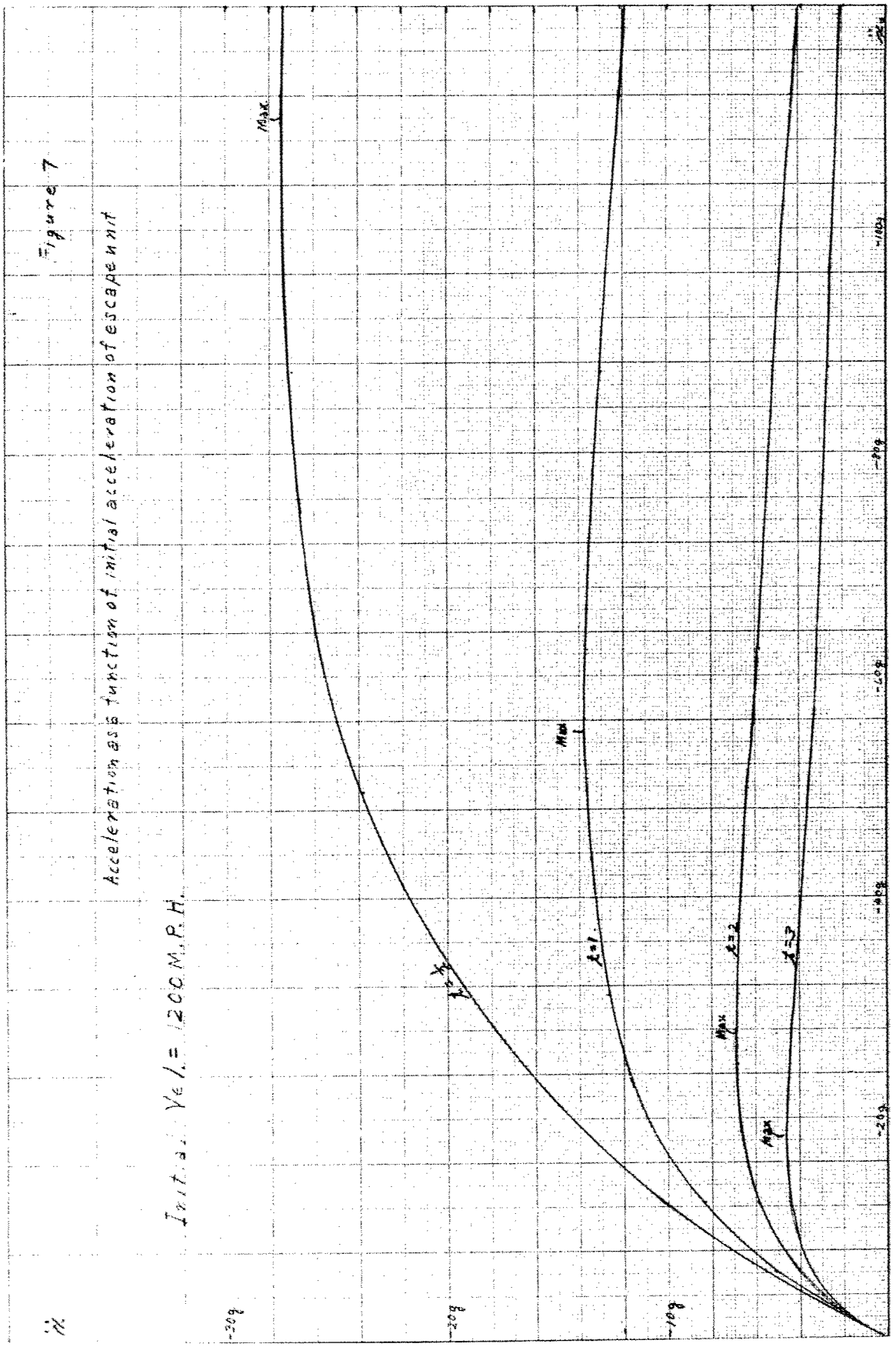
Figure 7
Acceleration as a function of initial acceleration of escapement
Init. s. Vel. = 120 M.P.H.
Max
Max
Max
Max
-30g
-20g
-10g
-40g
-50g
-60g
-70g
-80g
-90g
-100g
-110g
-120g
-130g
-140g
-150g
-160g
-170g
-180g
-190g
-200g
-210g
-220g
-230g
-240g
-250g
-260g
-270g
-280g
-290g
-300g
-310g
-320g
-330g
-340g
-350g
-360g
-370g
-380g
-390g
-400g
-410g
-420g
-430g
-440g
-450g
-460g
-470g
-480g
-490g
-500g
-510g
-520g
-530g
-540g
-550g
-560g
-570g
-580g
-590g
-600g
-610g
-620g
-630g
-640g
-650g
-660g
-670g
-680g
-690g
-700g
-710g
-720g
-730g
-740g
-750g
-760g
-770g
-780g
-790g
-800g
-810g
-820g
-830g
-840g
-850g
-860g
-870g
-880g
-890g
-900g
-910g
-920g
-930g
-940g
-950g
-960g
-970g
-980g
-990g
-1000g
-1010g
-1020g
-1030g
-1040g
-1050g
-1060g
-1070g
-1080g
-1090g
-1100g
-1110g
-1120g
-1130g
-1140g
-1150g
-1160g
-1170g
-1180g
-1190g
-1200g
-1210g
-1220g
-1230g
-1240g
-1250g
-1260g
-1270g
-1280g
-1290g
-1300g
-1310g
-1320g
-1330g
-1340g
-1350g
-1360g
-1370g
-1380g
-1390g
-1400g
-1410g
-1420g
-1430g
-1440g
-1450g
-1460g
-1470g
-1480g
-1490g
-1500g
-1510g
-1520g
-1530g
-1540g
-1550g
-1560g
-1570g
-1580g
-1590g
-1600g
-1610g
-1620g
-1630g
-1640g
-1650g
-1660g
-1670g
-1680g
-1690g
-1700g
-1710g
-1720g
-1730g
-1740g
-1750g
-1760g
-1770g
-1780g
-1790g
-1800g
-1810g
-1820g
-1830g
-1840g
-1850g
-1860g
-1870g
-1880g
-1890g
-1900g
-1910g
-1920g
-1930g
-1940g
-1950g
-1960g
-1970g
-1980g
-1990g
-2000g
-2010g
-2020g
-2030g
-2040g
-2050g
-2060g
-2070g
-2080g
-2090g
-2100g
-2110g
-2120g
-2130g
-2140g
-2150g
-2160g
-2170g
-2180g
-2190g
-2200g
-2210g
-2220g
-2230g
-2240g
-2250g
-2260g
-2270g
-2280g
-2290g
-2300g
-2310g
-2320g
-2330g
-2340g
-2350g
-2360g
-2370g
-2380g
-2390g
-2400g
-2410g
-2420g
-2430g
-2440g
-2450g
-2460g
-2470g
-2480g
-2490g
-2500g
-2510g
-2520g
-2530g
-2540g
-2550g
-2560g
-2570g
-2580g
-2590g
-2600g
-2610g
-2620g
-2630g
-2640g
-2650g
-2660g
-2670g
-2680g
-2690g
-2700g
-2710g
-2720g
-2730g
-2740g
-2750g
-2760g
-2770g
-2780g
-2790g
-2800g
-2810g
-2820g
-2830g
-2840g
-2850g
-2860g
-2870g
-2880g
-2890g
-2900g
-2910g
-2920g
-2930g
-2940g
-2950g
-2960g
-2970g
-2980g
-2990g
-3000g
-3010g
-3020g
-3030g
-3040g
-3050g
-3060g
-3070g
-3080g
-3090g
-3100g
-3110g
-3120g
-3130g
-3140g
-3150g
-3160g
-3170g
-3180g
-3190g
-3200g
-3210g
-3220g
-3230g
-3240g
-3250g
-3260g
-3270g
-3280g
-3290g
-3300g
-3310g
-3320g
-3330g
-3340g
-3350g
-3360g
-3370g
-3380g
-3390g
-3400g
-3410g
-3420g
-3430g
-3440g
-3450g
-3460g
-3470g
-3480g
-3490g
-3500g
-3510g
-3520g
-3530g
-3540g
-3550g
-3560g
-3570g
-3580g
-3590g
-3600g
-3610g
-3620g
-3630g
-3640g
-3650g
-3660g
-3670g
-3680g
-3690g
-3700g
-3710g
-3720g
-3730g
-3740g
-3750g
-3760g
-3770g
-3780g
-3790g
-3800g
-3810g
-3820g
-3830g
-3840g
-3850g
-3860g
-3870g
-3880g
-3890g
-3900g
-3910g
-3920g
-3930g
-3940g
-3950g
-3960g
-3970g
-3980g
-3990g
-4000g
-4010g
-4020g
-4030g
-4040g
-4050g
-4060g
-4070g
-4080g
-4090g
-4100g
-4110g
-4120g
-4130g
-4140g
-4150g
-4160g
-4170g
-4180g
-4190g
-4200g
-4210g
-4220g
-4230g
-4240g
-4250g
-4260g
-4270g
-4280g
-4290g
-4300g
-4310g
-4320g
-4330g
-4340g
-4350g
-4360g
-4370g
-4380g
-4390g
-4400g
-4410g
-4420g
-4430g
-4440g
-4450g
-4460g
-4470g
-4480g
-4490g
-4500g
-4510g
-4520g
-4530g
-4540g
-4550g
-4560g
-4570g
-4580g
-4590g
-4600g
-4610g
-4620g
-4630g
-4640g
-4650g
-4660g
-4670g
-4680g
-4690g
-4700g
-4710g
-4720g
-4730g
-4740g
-4750g
-4760g
-4770g
-4780g
-4790g
-4800g
-4810g
-4820g
-4830g
-4840g
-4850g
-4860g
-4870g
-4880g
-4890g
-4900g
-4910g
-4920g
-4930g
-4940g
-4950g
-4960g
-4970g
-4980g
-4990g
-5000g
-5010g
-5020g
-5030g
-5040g
-5050g
-5060g
-5070g
-5080g
-5090g
-5100g
-5110g
-5120g
-5130g
-5140g
-5150g
-5160g
-5170g
-5180g
-5190g
-5200g
-5210g
-5220g
-5230g
-5240g
-5250g
-5260g
-5270g
-5280g
-5290g
-5300g
-5310g
-5320g
-5330g
-5340g
-5350g
-5360g
-5370g
-5380g
-5390g
-5400g
-5410g
-5420g
-5430g
-5440g
-5450g
-5460g
-5470g
-5480g
-5490g
-5500g
-5510g
-5520g
-5530g
-5540g
-5550g
-5560g
-5570g
-5580g
-5590g
-5600g
-5610g
-5620g
-5630g
-5640g
-5650g
-5660g
-5670g
-5680g
-5690g
-5700g
-5710g
-5720g
-5730g
-5740g
-5750g
-5760g
-5770g
-5780g
-5790g
-5800g
-5810g
-5820g
-5830g
-5840g
-5850g
-5860g
-5870g
-5880g
-5890g
-5900g
-5910g
-5920g
-5930g
-5940g
-5950g
-5960g
-5970g
-5980g
-5990g
-6000g
-6010g
-6020g
-6030g
-6040g
-6050g
-6060g
-6070g
-6080g
-6090g
-6100g
-6110g
-6120g
-6130g
-6140g
-6150g
-6160g
-6170g
-6180g
-6190g
-6200g
-6210g
-6220g
-6230g
-6240g
-6250g
-6260g
-6270g
-6280g
-6290g
-6300g
-6310g
-6320g
-6330g
-6340g
-6350g
-6360g
-6370g
-6380g
-6390g
-6400g
-6410g
-6420g
-6430g
-6440g
-6450g
-6460g
-6470g
-6480g
-6490g
-6500g
-6510g
-6520g
-6530g
-6540g
-6550g
-6560g
-6570g
-6580g
-6590g
-6600g
-6610g
-6620g
-6630g
-6640g
-6650g
-6660g
-6670g
-6680g
-6690g
-6700g
-6710g
-6720g
-6730g
-6740g
-6750g
-6760g
-6770g
-6780g
-6790g
-6800g
-6810g
-6820g
-6830g
-6840g
-6850g
-6860g
-6870g
-6880g
-6890g
-6900g
-6910g
-6920g
-6930g
-6940g
-6950g
-6960g
-6970g
-6980g
-6990g
-7000g
-7010g
-7020g
-7030g
-7040g
-7050g
-7060g
-7070g
-7080g
-7090g
-7100g
-7110g
-7120g
-7130g
-7140g
-7150g
-7160g
-7170g
-7180g
-7190g
-7200g
-7210g
-7220g
-7230g
-7240g
-7250g
-7260g
-7270g
-7280g
-7290g
-7300g
-7310g
-7320g
-7330g
-7340g
-7350g
-7360g
-7370g
-7380g
-7390g
-7400g
-7410g
-7420g
-7430g
-7440g
-7450g
-7460g
-7470g
-7480g
-7490g
-7500g
-7510g
-7520g
-7530g
-7540g
-7550g
-7560g
-7570g
-7580g
-7590g
-7600g
-7610g
-7620g
-7630g
-7640g
-7650g
-7660g
-7670g
-7680g
-7690g
-7700g
-7710g
-7720g
-7730g
-7740g
-7750g
-7760g
-7770g
-7780g
-7790g
-7800g
-7810g
-7820g
-7830g
-7840g
-7850g
-7860g
-7870g
-7880g
-7890g
-7900g
-7910g
-7920g
-7930g
-7940g
-7950g
-7960g
-7970g
-7980g
-7990g
-8000g
-8010g
-8020g
-8030g
-8040g
-8050g
-8060g
-8070g
-8080g
-8090g
-8100g
-8110g
-8120g
-8130g
-8140g
-8150g
-8160g
-8170g
-8180g
-8190g
-8200g
-8210g
-8220g
-8230g
-8240g
-8250g
-8260g
-8270g
-8280g
-8290g
-8300g
-8310g
-8320g
-8330g
-8340g
-8350g
-8360g
-8370g
-8380g
-8390g
-8400g
-8410g
-8420g
-8430g
-8440g
-8450g
-8460g
-8470g
-8480g
-8490g
-8500g
-8510g
-8520g
-8530g
-8540g
-8550g
-8560g
-8570g
-8580g
-8590g
-8600g
-8610g
-8620g
-8630g
-8640g
-8650g
-8660g
-8670g
-8680g
-8690g
-8700g
-8710g
-8720g
-8730g
-8740g
-8750g
-8760g
-8770g
-8780g
-8790g
-8800g
-8810g
-8820g
-8830g
-8840g
-8850g
-8860g
-8870g
-8880g
-8890g
-8900g
-8910g
-8920g
-8930g
-8940g
-8950g
-8960g
-8970g
-8980g
-8990g
-9000g
-9010g
-9020g
-9030g
-9040g
-9050g
-9060g
-9070g
-9080g
-9090g
-9100g
-9110g
-9120g
-9130g
-9140g
-9150g
-9160g
-9170g
-9180g
-9190g
-9200g
-9210g
-9220g
-9230g
-9240g
-9250g
-9260g
-9270g
-9280g
-9290g
-9300g
-9310g
-9320g
-9330g
-9340g
-9350g
-9360g
-9370g
-9380g
-9390g
-9400g
-9410g
-9420g
-9430g
-9440g
-9450g
-9460g
-9470g
-9480g
-9490g
-9500g
-9510g
-9520g
-9530g
-9540g
-9550g
-9560g
-9570g
-9580g
-9590g
-9600g
-9610g
-9620g
-9630g
-9640g
-9650g
-9660g
-9670g
-9680g
-9690g
-9700g
-9710g
-9720g
-9730g
-9740g
-9750g
-9760g
-9770g
-9780g
-9790g
-9800g
-9810g
-9820g
-9830g
-9840g
-9850g
-9860g
-9870g
-9880g
-9890g
-9900g
-9910g
-9920g
-9930g
-9940g
-9950g
-9960g
-9970g
-9980g
-9990g
-10000g

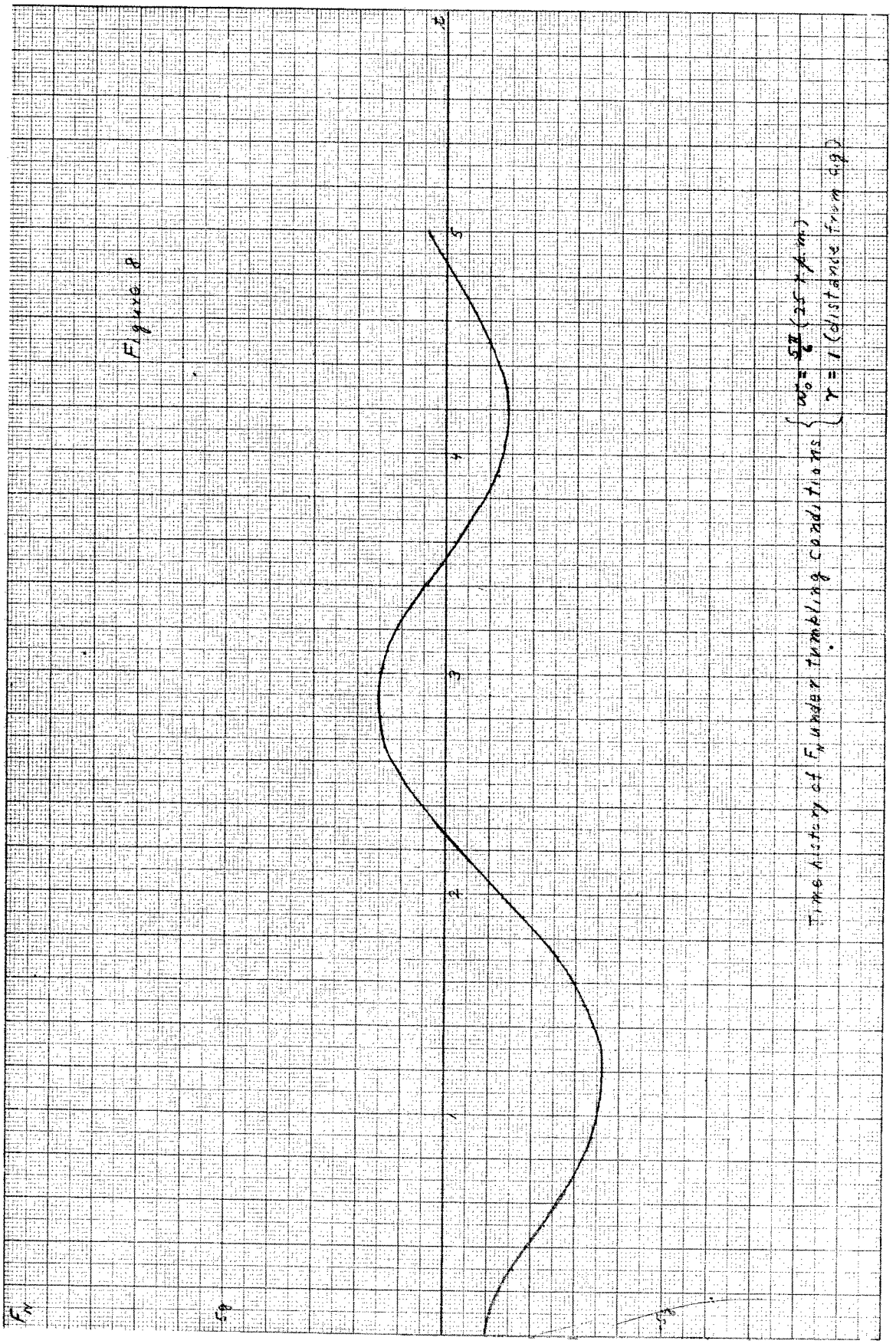
Figure 8
Time history of F_N under two-pulse combination
$\omega_0 = \frac{2\pi}{t_2}$ (2.5 cycles)
$\gamma = 1$ (Obtained from Fig. 4.8)
F_N
$\omega_0 t$

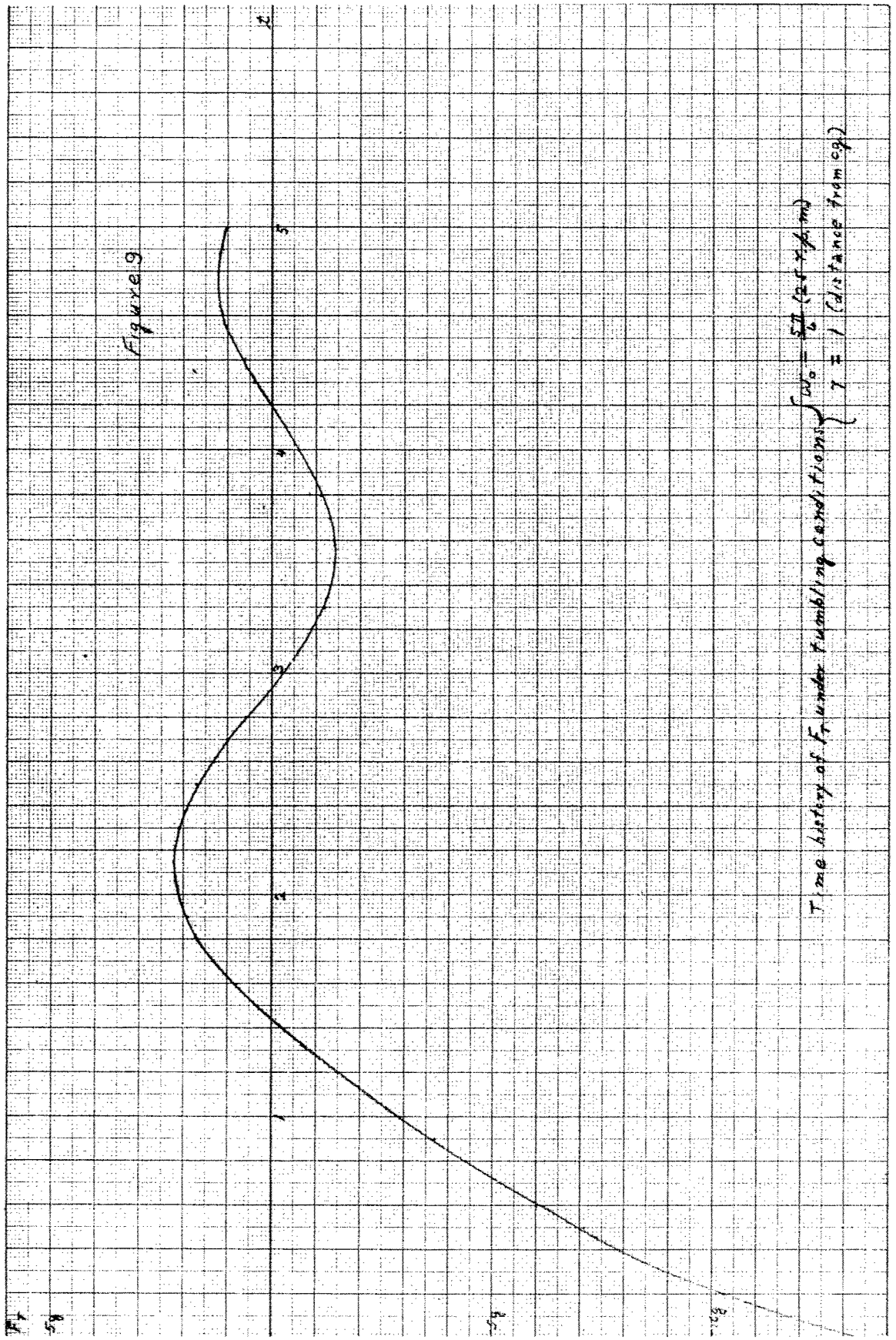
Figure 9
Time history of F_T under Rumbling Load Fluctuations
$\omega_0 = \frac{2\pi}{\lambda}$ (2πf/ω_m)
$\tau = f$ (distance from eg.)
F_T
τ
1
2
3
4
5

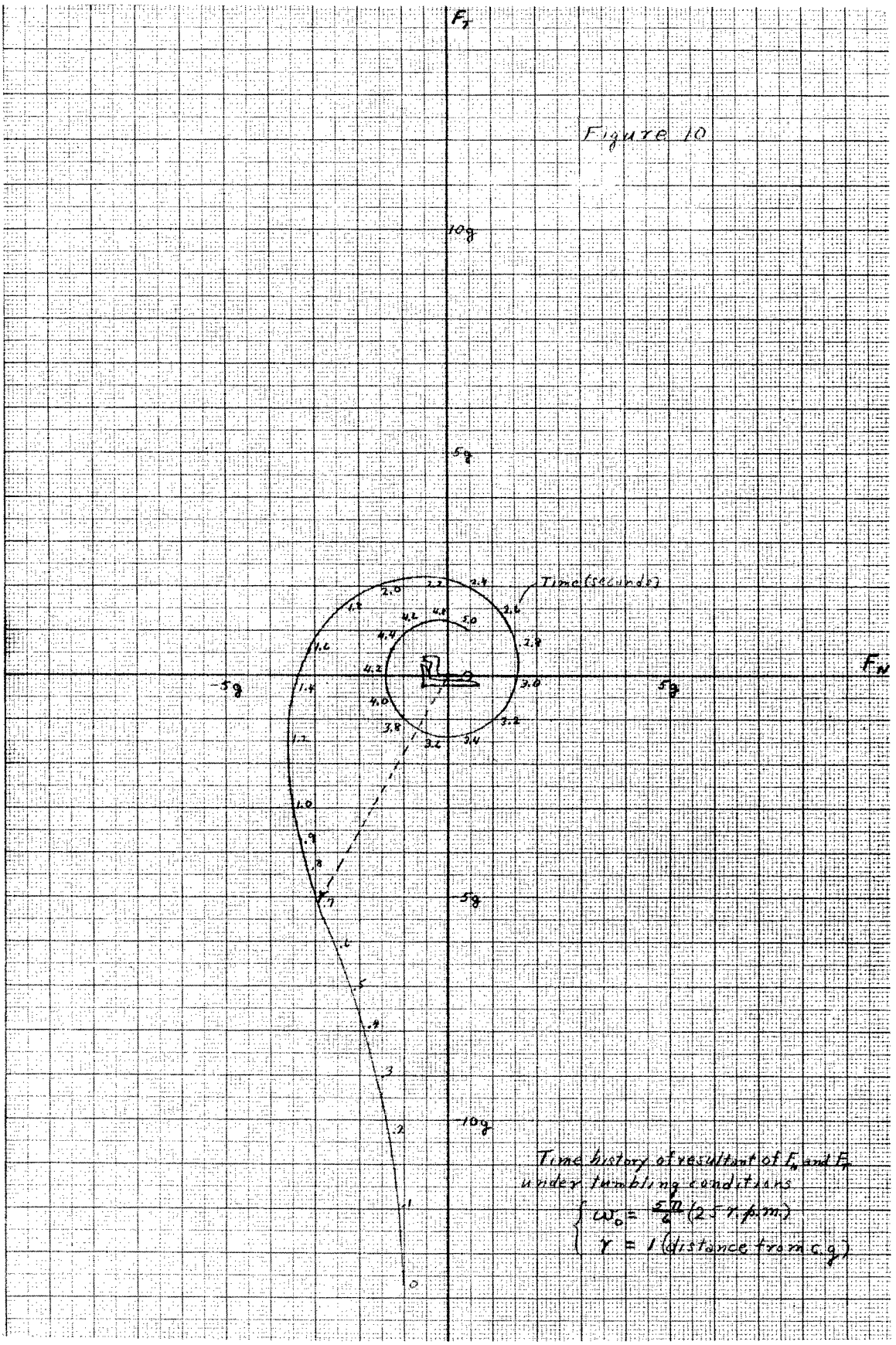

Figure 10

Time history of resultant of F_N and F_T under tumbling conditions

$\omega_0 = \frac{5\pi}{2}$ (2.5 r.p.m.)

$\gamma = 1$ (distance from c.g.)

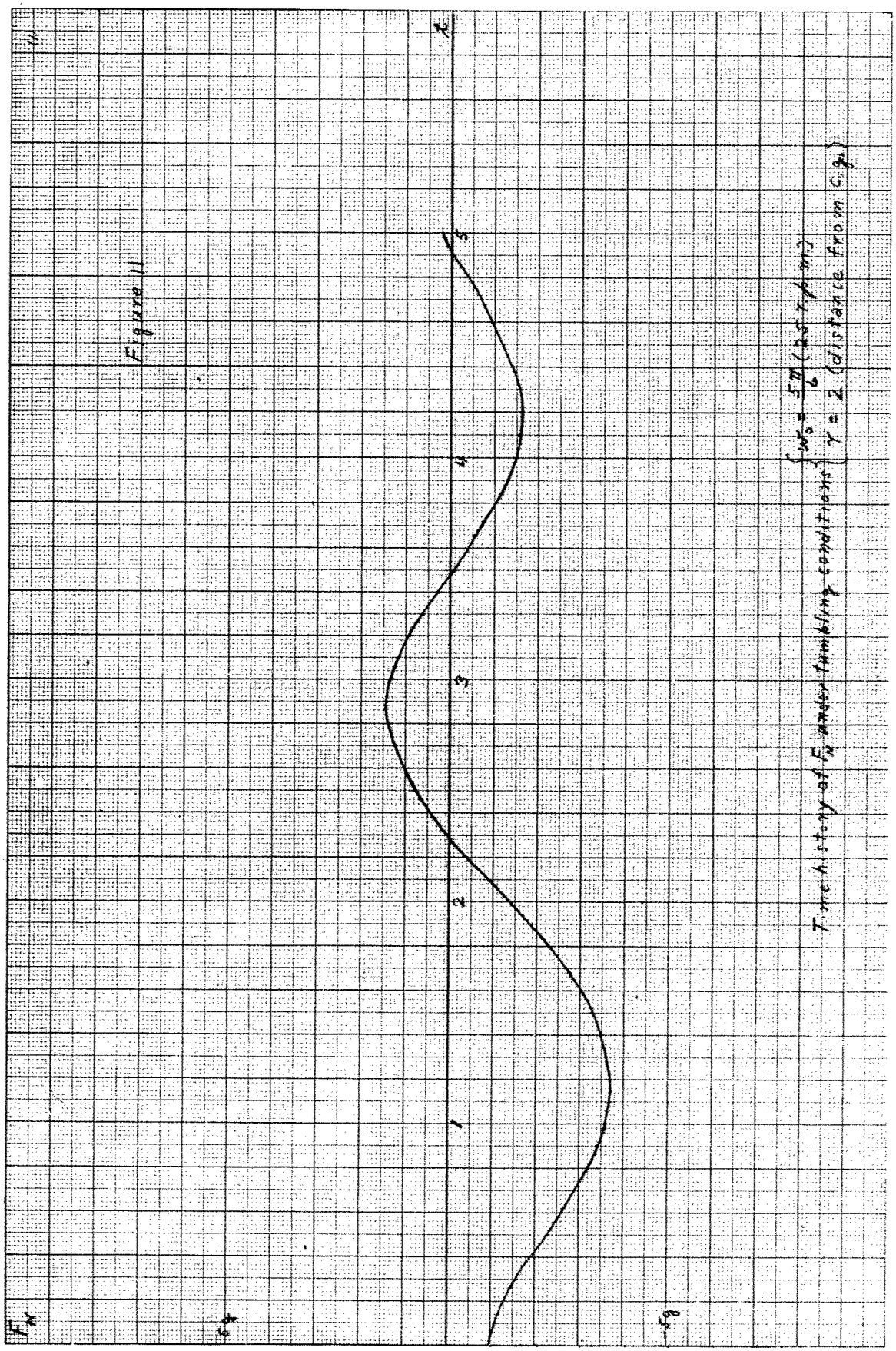
Figure 11
Fx
5
4
3
2
1
0
-.4
-.8
Theoretical variation of Fx under translational oscillations
(ωs = 5π/6 (see text) γ = 2 (distance from C.G.)

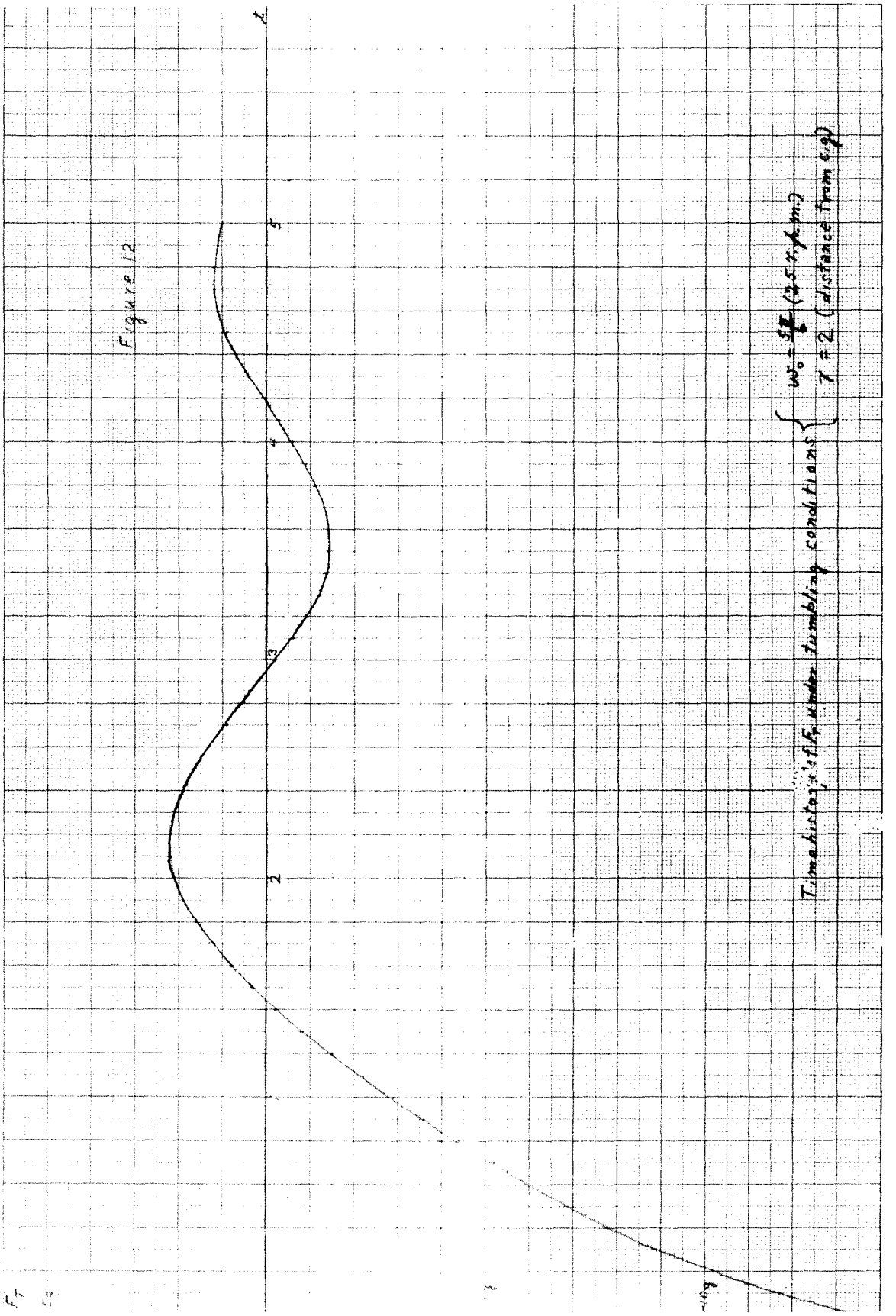
t
5
4
3
2
Figure 12
Time history of F under tumbling conditions
$W_0 = \frac{2\pi}{T}$ (2.5 yr. min.)
T = 2 (distance from c.g.)

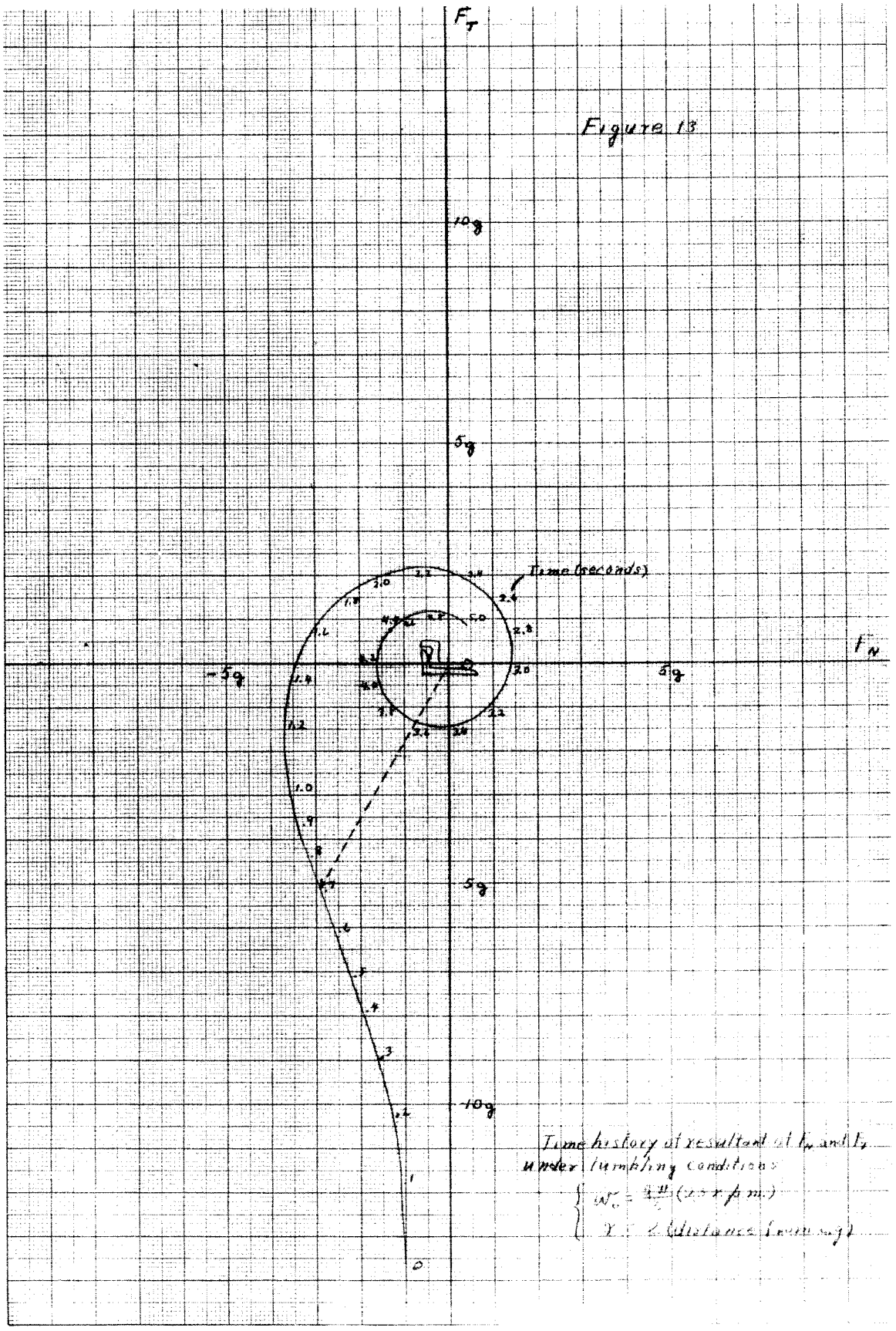

Figure 13

Time history of resultant of F_N and F_T under tumbling conditions

$W_c = \frac{4}{3}\pi$ (cm)

γ = (distance from c.g.)

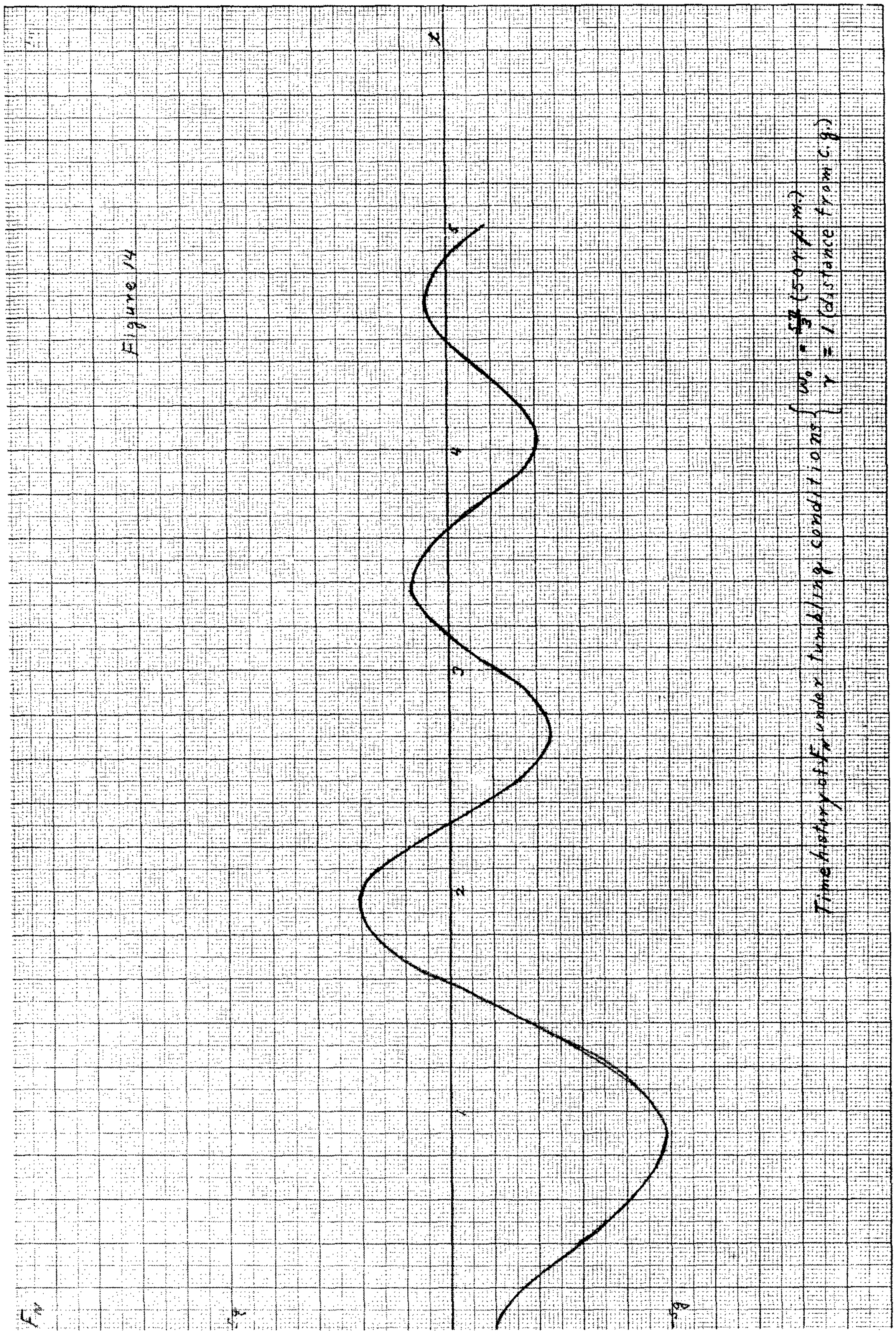
Figure 14
Time history of F_N under tumbling conditions
$\omega_0 = \frac{5\pi}{3}$ (50 r.p.m.)
$r = 1$ (distance from c.g.)
t
1
2
3
4
5
F_N

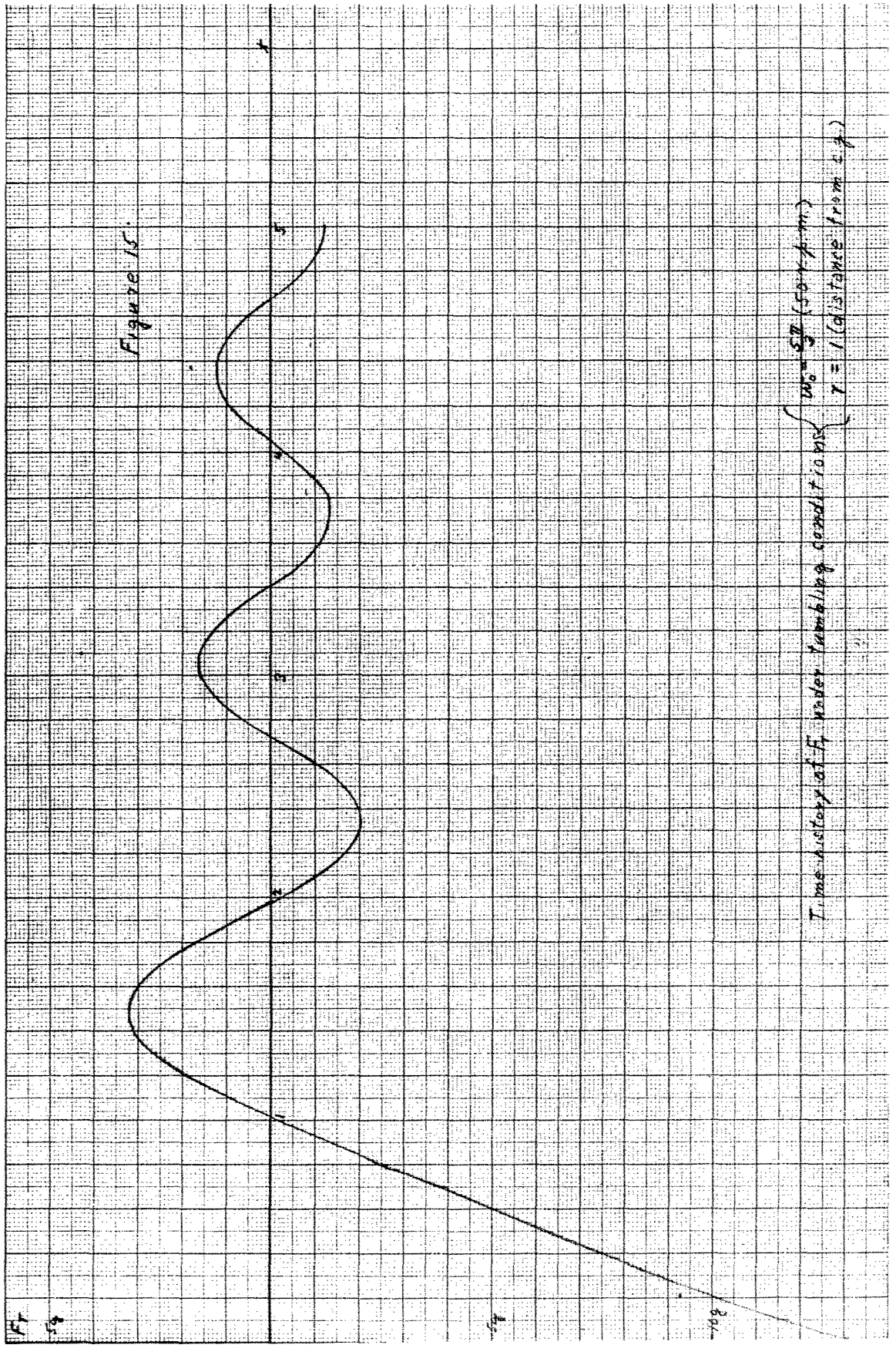
Figure 15.
Time history of F_T under impulse loading condition
$\omega_0 = \sqrt{\frac{k}{m}}$ (Equivalent)
$T = 1$ (distance from c.g.)
F_T
F_4
$-F_4$
$-\frac{mg}{k}$

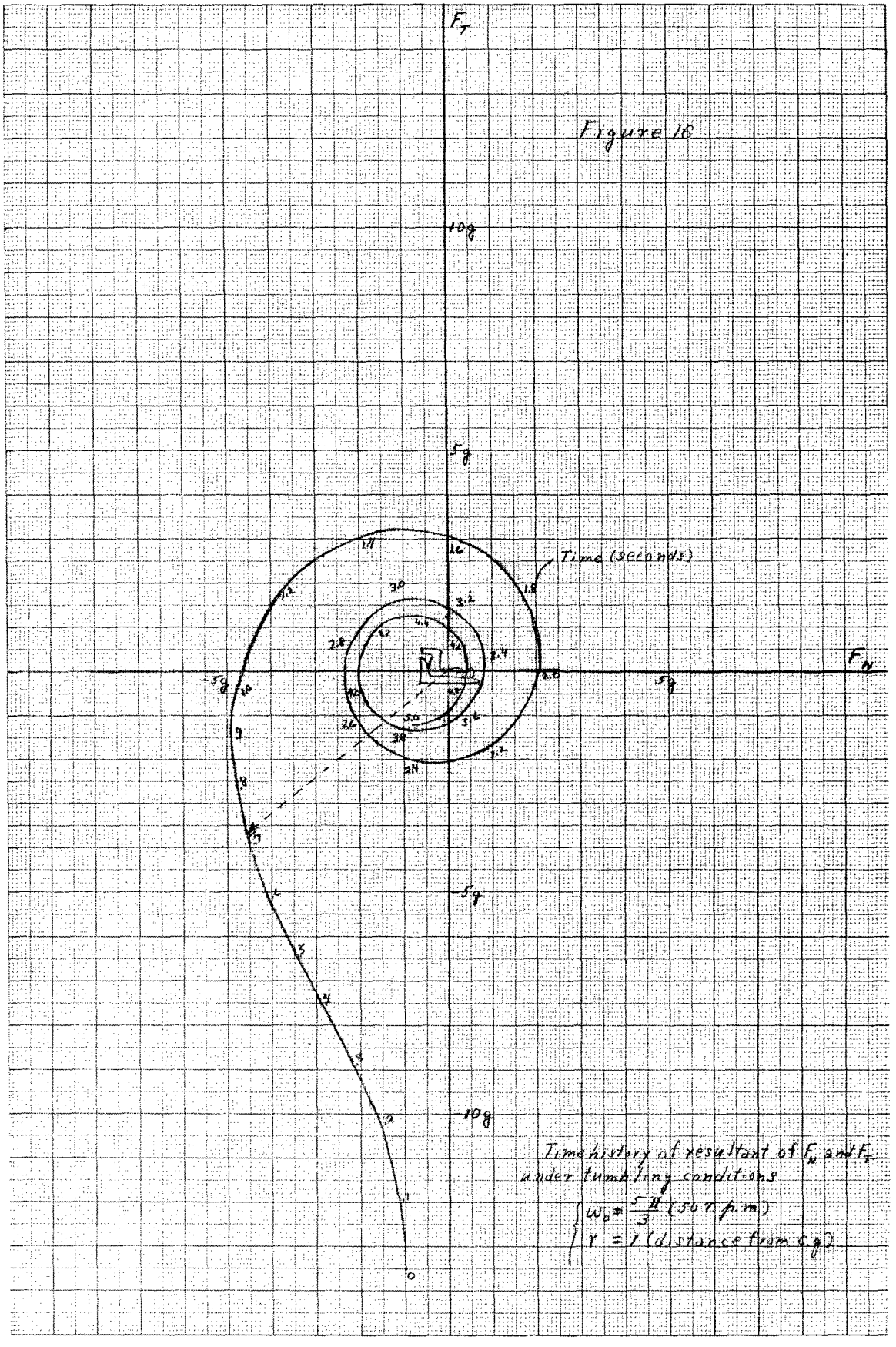

Figure 18

Time history of resultant of F_N and F_T under tumbling conditions

$\omega_0 = \frac{5\pi}{3}$ (50% p.m.)

γ = 1 (distance from c.g.)

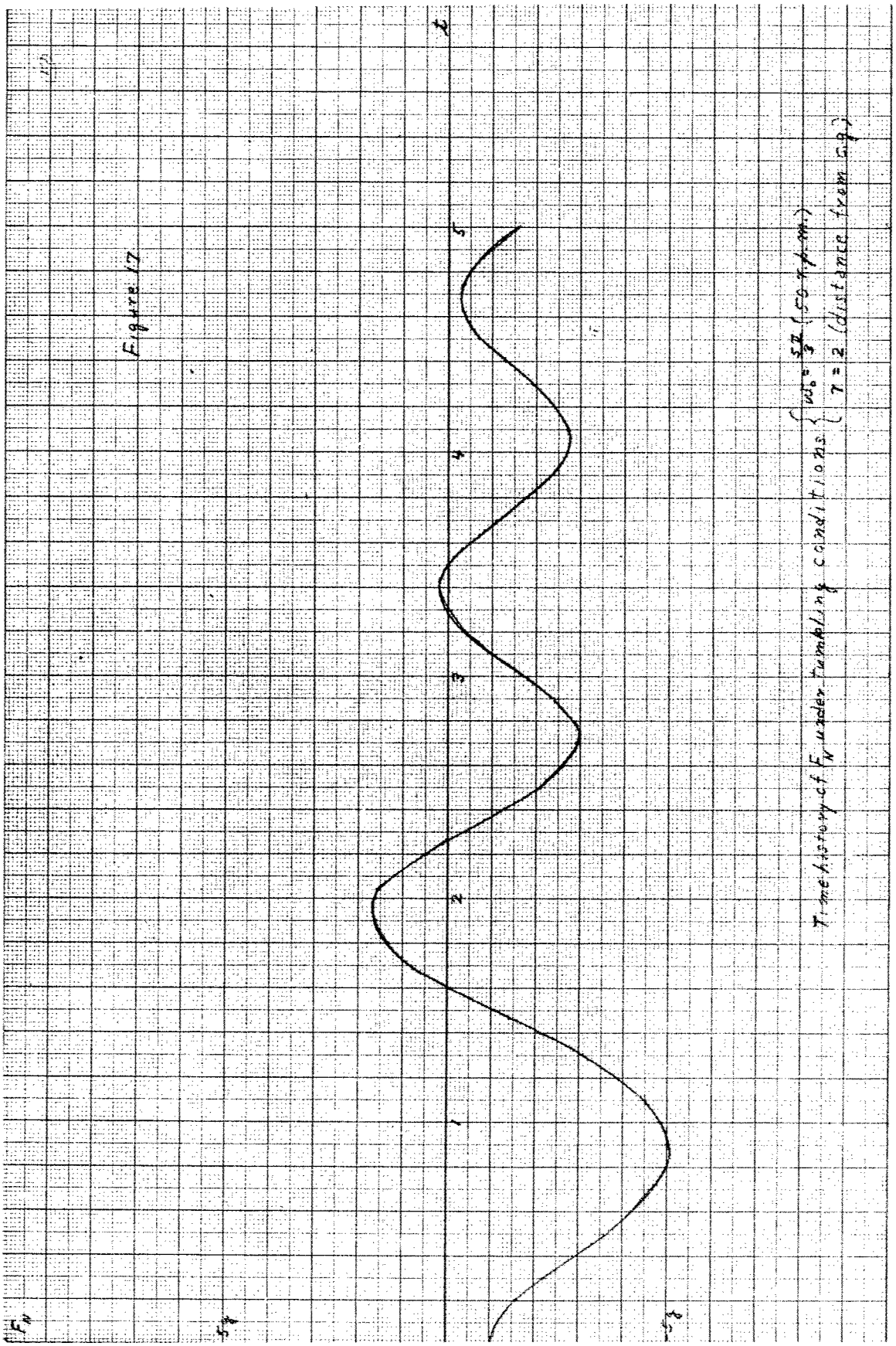
Figure 17
Time history of F_N under transient conditions ($\omega_0 = \frac{5\pi}{3}$ (cycles per min.) $\tau = 2$ (distance from C.G.))
F_N
F_A
F_B
1
2
3
4
5

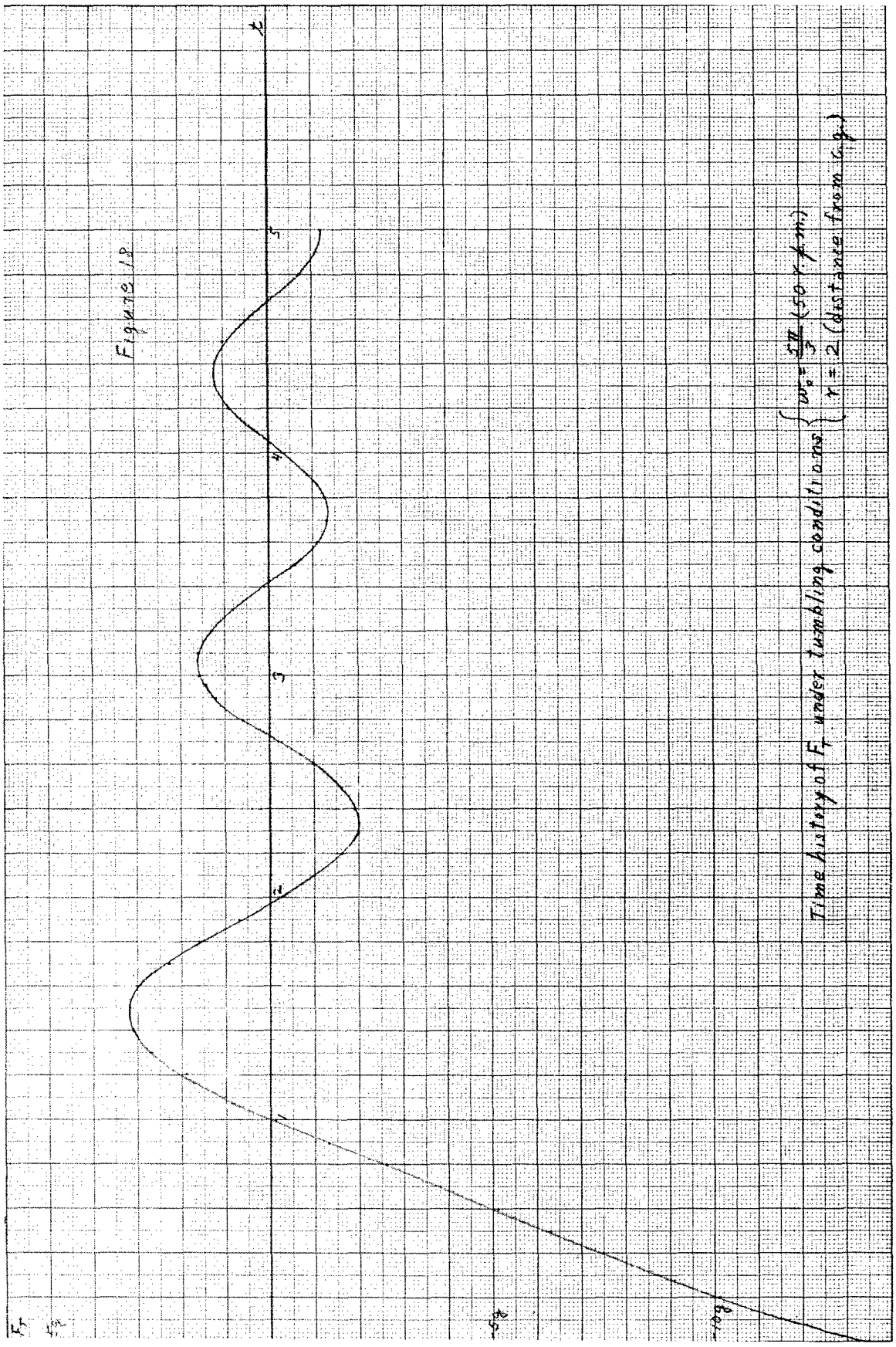

Figure 18

Time history of F_T under tumbling conditions $\left\{ \begin{array}{l} \omega_o = \frac{5\pi}{3} \text{ (50 r.p.m.)} \\ r = 2 \text{ (distance from c.g.)} \end{array} \right.$

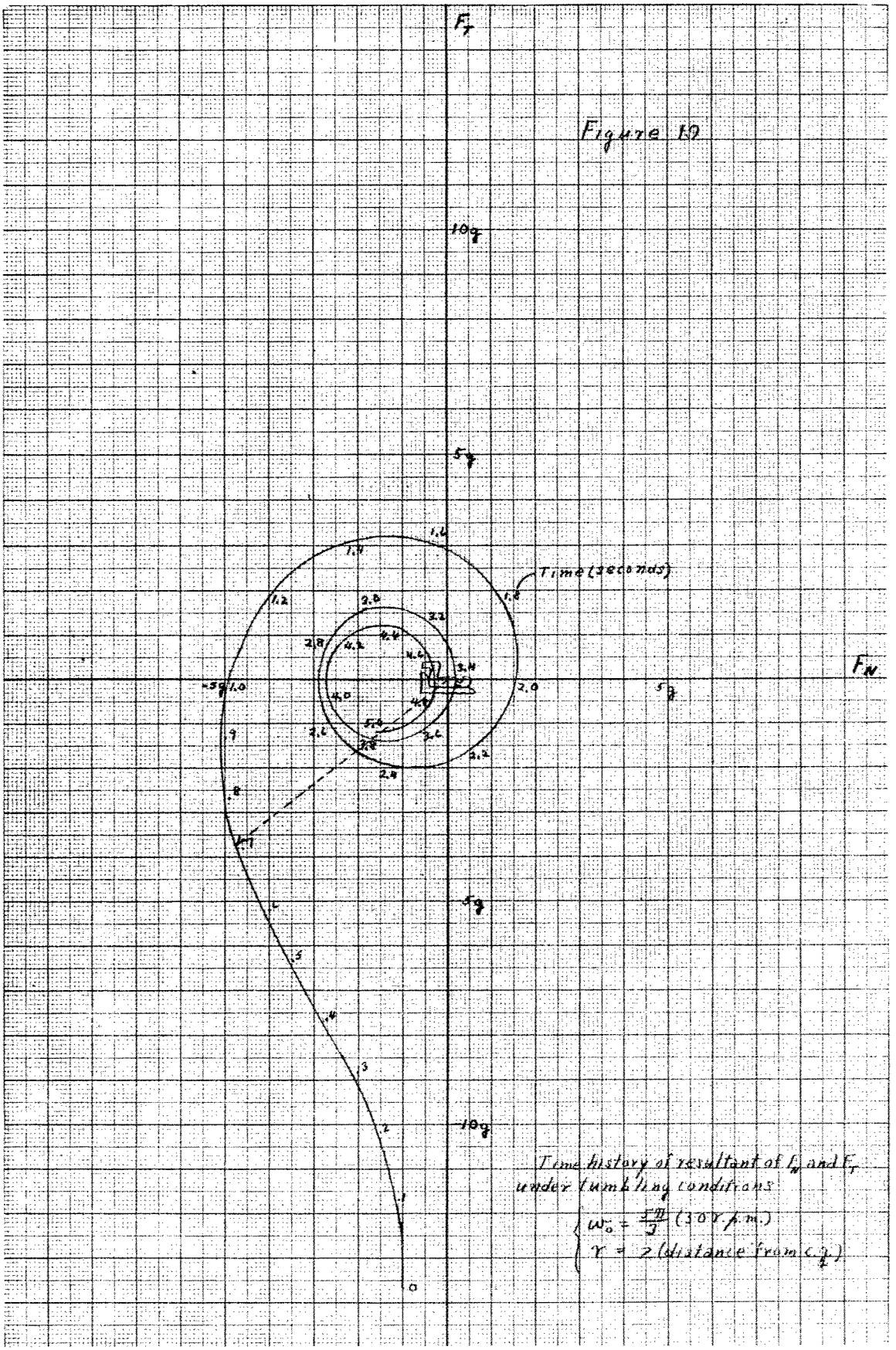

Figure 10

Time history of resultant of F_N and F_T under tumbling conditions

$\omega_0 = \frac{\pi}{2}$ (30 r.p.m.)

r = 2 (distance from c.g.)

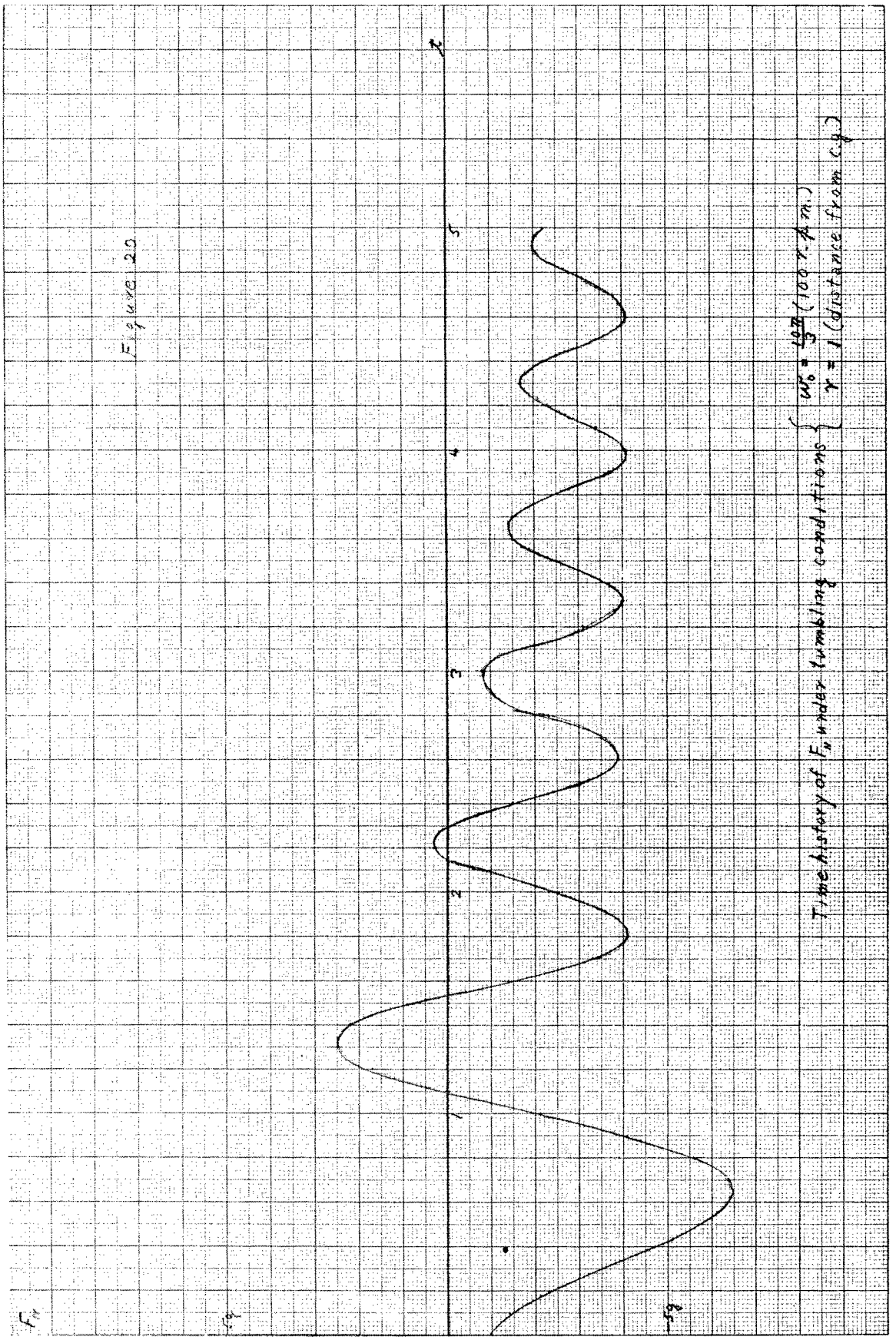
Time history of F_w under typical gust conditions $\left\{ \begin{array}{l} W_o = \frac{10T}{3} \text{ (100 ft. p.s.i.)} \\ r = 1 \text{ (distance from c.g.)} \end{array} \right.$
F_w
$\frac{F_w}{W_o}$
$\frac{t}{T}$
1
2
3
4
5
$\frac{t}{T}$ axis 2.0

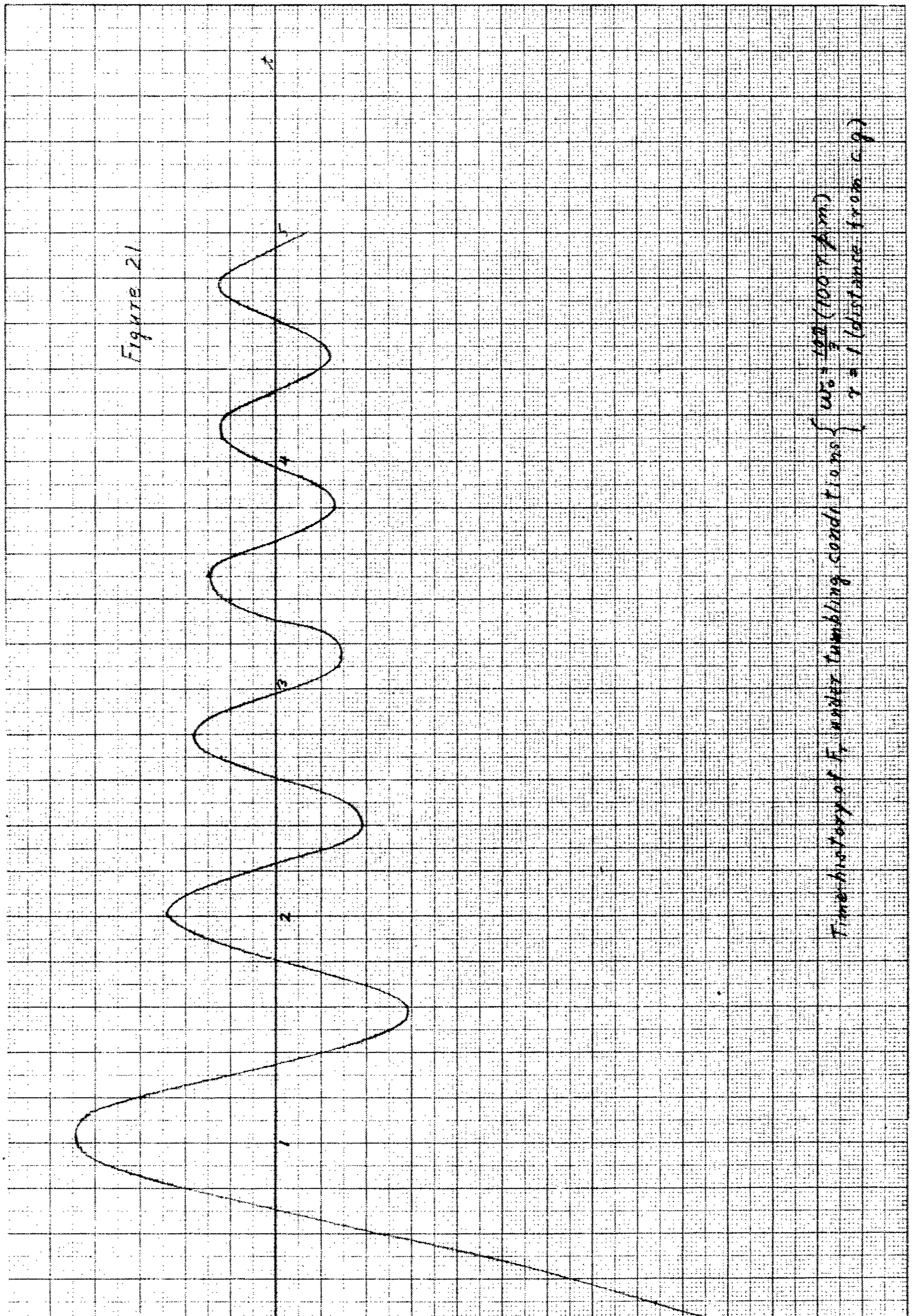
Figure 21
Time history of F_r under tumbling conditions $\left\{ \omega_0 = \frac{100}{3} \text{ (1000 rpm)}; \; r = 1 \text{ (distance from c.g.)} \right.$
1
2
3
4
5
t
F_r

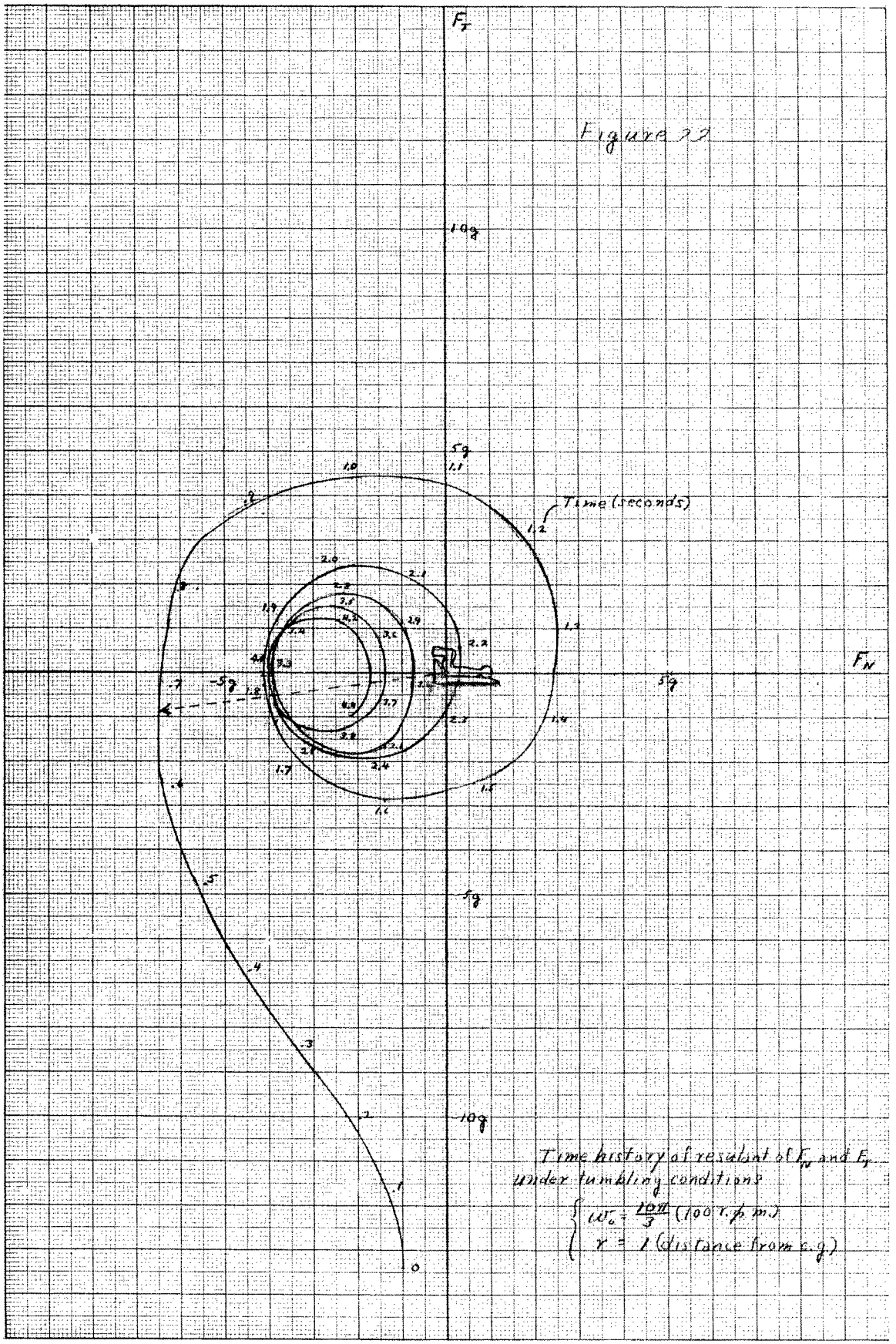

Figure 22

Time history of resultant of F_N and F_T under tumbling conditions

$\begin{cases} \omega_0 = \frac{10\pi}{3} \text{ (100 r.p.m.)} \\ r = 1 \text{ (distance from c.g.)} \end{cases}$

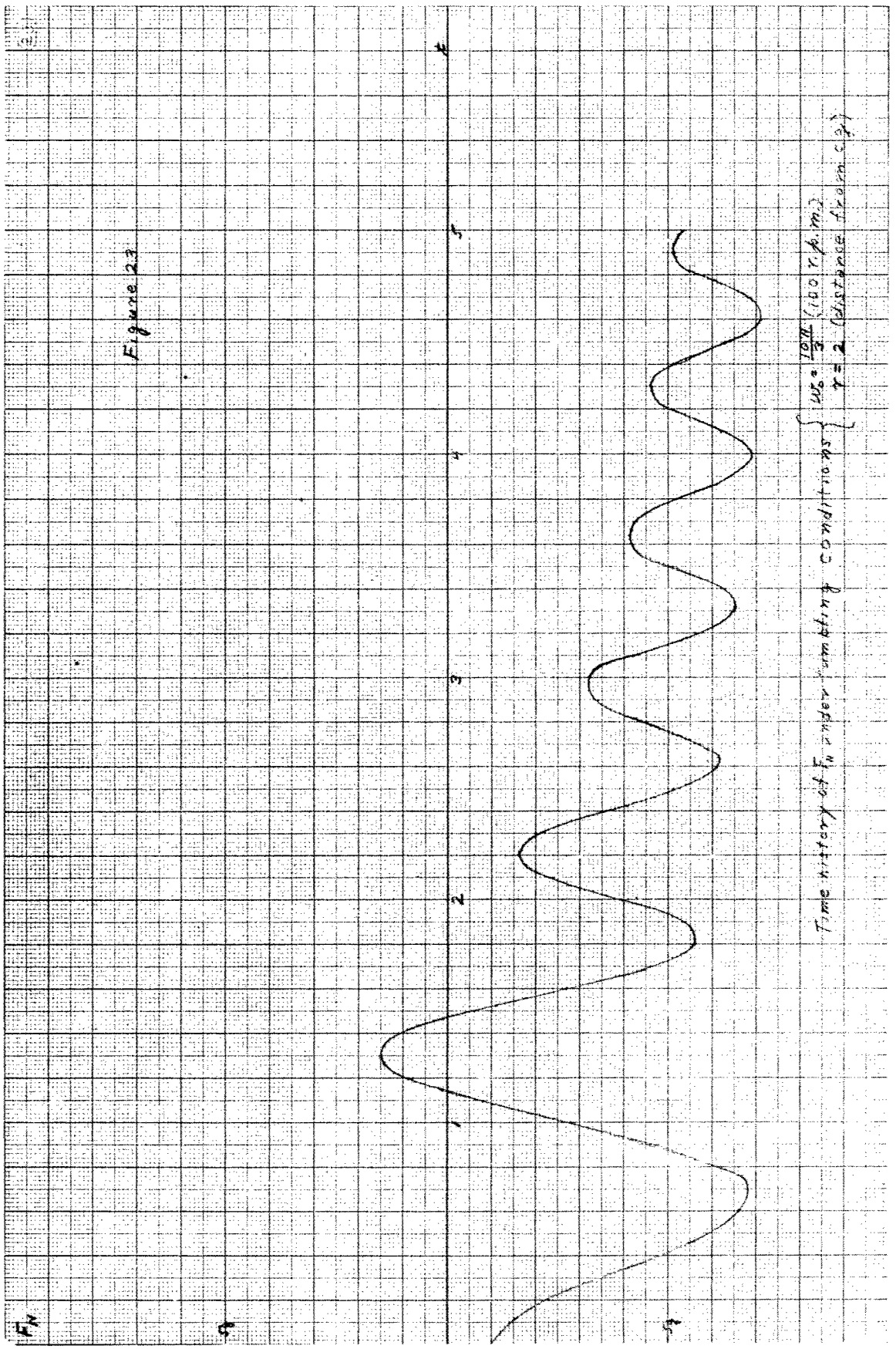
Figure 2.3
F_N
ϕ_N
$-\phi_N$
1
2
3
4
5
t
Time history of F_N when ϕ_N varies with a constant ω_s
$\omega_s = \frac{10\pi}{3}$ (100 r.p.m.)
$\tau = 2$ (distance from cg)

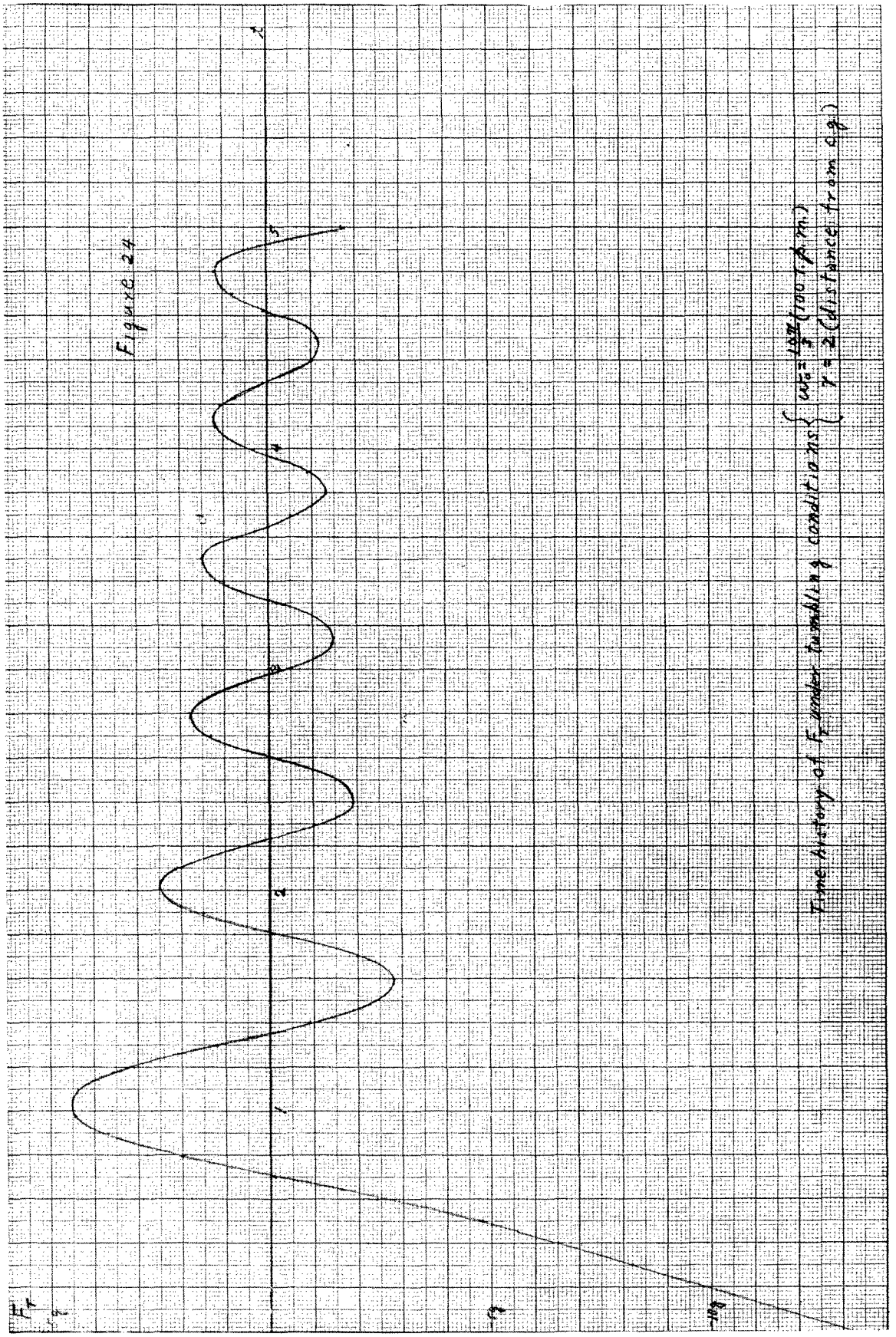
Figure 24
Time history of F under tumbling conditions (ω_a = 10π (rad/μ sec)
γ = 2 (distance from C.g.)
F
t
1
2
3
4
5
-log

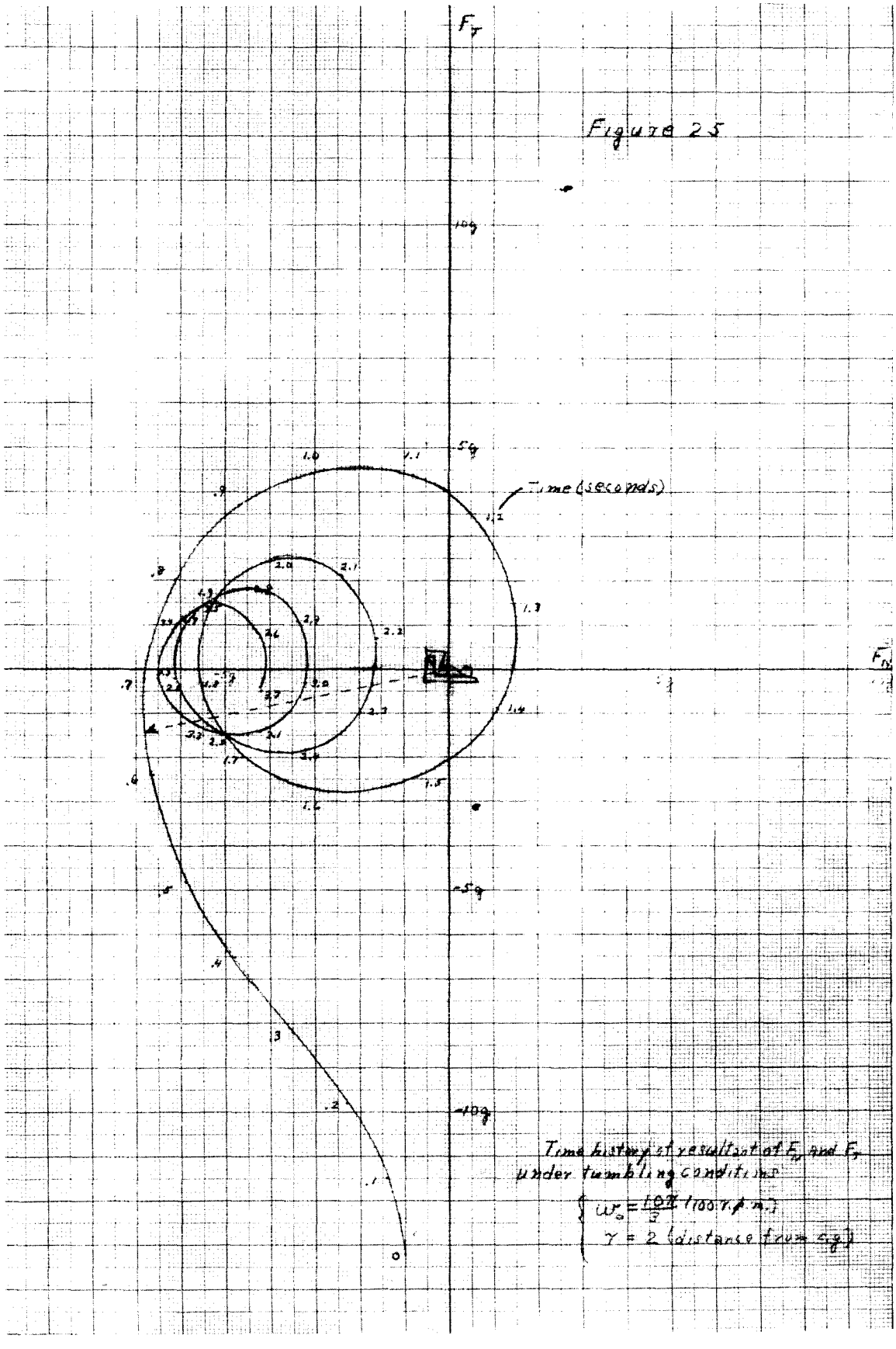

Figure 25

Time history of results of F_N and F_T under tumbling conditions

$\omega_o = \frac{10\pi}{3}$ (100 r.p.m.)

$\gamma = 2$ (distance from c.g.)

DISTRIBUTION LIST

WCAPP (2)
BAGR (4)
WCRDB (4)
WCLS (4)
WCLE (1)
WCRRM (10)
ASTIA (2)

Director of Research and Development
Headquarters, USAF
Attn: Col. A. P. Gagge
Washington 25, D. C.

Director
Air University Library
Maxwell Air Force Base, Alabama

Director
U.S. Naval Research Laboratory
Attn: Code 2021
Washington 25, D. C.

Bell Aircraft Corp.
Attn: Librarian
Niagara Falls 7, New York

Boeing Airplane Company
Attn: F. C. Taylor, Librarian
Wichita, Kansas

Boeing Airplane Company
Attn: Librarian
Seattle 14, Washington

Consolidated Vultee Aircraft Corp.
Attn: J. W. Larson
Thru: AFPR
Fort Worth, Texas

Consolidated Vultee Aircraft Corp.
Attn: Librarian
San Diego, California

Douglas Aircraft Company, Inc.
Attn: Librarian
El Segundo, California

Douglas Aircraft Company, Inc.
Attn: Librarian
Santa Monica, California

Fairchild Engine & Airplane Corp.
Attn: Librarian
Hagerstown, Maryland

Goodyear Aircraft Corp.
Attn: Librarian
Akron, Ohio

Glen L. Martin Company
Attn: Librarian
Baltimore 3, Maryland

Grumman Aircraft Engineering Corp.
Attn: Librarian
Bethpage, Long Island, New York

Lockheed Aircraft Corp.
Attn: Librarian
Burbank, California

McDonnel Aircraft Corp.
Attn: Librarian
St. Louis 21, Missouri

National Advisory Committee for Aeronautics
1724 F St., N.W.
Washington, D. C.

North American Aviation, Inc.
Attn: Librarian
Los Angeles 45, California

Northrop Aircraft Inc.
Attn: Librarian
Hawthorne, California

Republic Aircraft Corp.
Attn: Librarian
Farmingdale, Long Island, New York

Stanley Aviation Corp.
1560 Harlem Road
Attn: Librarian
Buffalo 6, New York